

Update in the Evaluation of the Solitary Pulmonary Nodule¹

Mylene T. Truong, MD
Jane P. Ko, MD
Santiago E. Rossi, MD
Ignacio Rossi, MD
Chitra Viswanathan, MD
John F. Bruzzi, MBBSCh
Edith M. Marom, MD
Jeremy J. Erasmus, MD

Abbreviations: AAH = atypical adenomatous hyperplasia, ACCP = American College of Chest Physicians, AIS = adenocarcinoma in situ, ATS = American Thoracic Society, BAC = bronchioloalveolar carcinoma, CAD = computer-aided diagnosis, ERS = European Respiratory Society, FDG = fluorodeoxyglucose, GGAN = ground-glass-attenuation nodule, IASLC = International Association for the Study of Lung Cancer, LPA = lepidic-predominant adenocarcinoma, MDCT = multidetector CT, MIA = minimally invasive adenocarcinoma, PSN = partly solid nodule, SPN = solitary pulmonary nodule, SSN = solitary subsolid nodule, SUV = standardized uptake value

RadioGraphics 2014; 34:1658–1679

Published online 10.1148/rg.346130092

Content Codes:   

¹From the Department of Radiology, University of Texas MD Anderson Cancer Center, 1515 Holcombe Blvd, Unit 1478, Houston, TX 77030 (M.T.T., C.V., E.M.M., J.J.E.); Department of Radiology, New York University Langone Medical Center, New York, NY (J.P.K.); Department of Radiology, Centro de Diagnóstico Dr Enrique Rossi, Buenos Aires, Argentina (S.E.R., I.R.); and Department of Radiology, University College Hospital Galway, Galway, Ireland (J.F.B.). Recipient of a Magna Cum Laude award for an education exhibit at the 2012 RSNA Annual Meeting. Received June 20, 2013; revision requested September 24 and received October 1; accepted October 19. For this journal-based SA-CME activity, the author S.E.R. has provided a disclosure (see p 1677); all other authors, the editor, and the reviewers have disclosed no relevant relationships. **Address correspondence** to M.T.T. (e-mail: mtruong@mdanderson.org).

SA-CME LEARNING OBJECTIVES

After completing this journal-based SA-CME activity, participants will be able to:

- Identify CT features of subsolid lesions that are indicative of an increased risk for malignancy.
- List the differential diagnosis of solid and subsolid solitary pulmonary nodules.
- Discuss the treatment and follow-up of patients with a solitary pulmonary nodule.

See www.rsna.org/education/search/RG.

A solitary pulmonary nodule (SPN) is defined as a round opacity that is smaller than 3 cm. It may be solid or subsolid in attenuation. Semisolid nodules may have purely ground-glass attenuation or be partly solid (mixed solid and ground-glass attenuation). The widespread use of multidetector computed tomography (CT) has increased the detection of SPNs. Although clinical assessment of patients' risk factors for malignancy—such as age, smoking history, and history of malignancy—is important to determine appropriate treatment, in the recently published Fleischner guidelines for subsolid nodules, smoking history does not factor into their recommendations for management because there is an increasing incidence of lung adenocarcinoma in younger and nonsmoking patients. At imaging evaluation, obtaining prior chest radiographs or CT images is useful to assess nodule growth. Further imaging evaluation, including CT enhancement studies and positron emission tomography (PET), helps determine the malignant potential of solid SPNs. For subsolid nodules, initial follow-up CT is performed at 3 months to determine persistence, because lesions with an infectious or inflammatory cause can resolve in the interval. CT enhancement studies are not applicable for subsolid nodules, and PET is of limited utility because of the low metabolic activity of these lesions. Because of the likelihood that persistent subsolid nodules represent adenocarcinoma with indolent growth, serial imaging reassessment for a minimum of 3 years and/or obtaining tissue samples for histologic analysis are recommended. In the follow-up of subsolid SPNs, imaging features that indicate an increased risk for malignancy include an increase in size, an increase in attenuation, and development of a solid component.

©RSNA, 2014 • radiographics.rsna.org

Introduction

A solitary pulmonary nodule (SPN) is defined as a round opacity that is at least moderately well margined and no larger than 3 cm in its maximum diameter (1). The adjective *small* has been used to describe nodules that are less than 1 cm in diameter (1). Small nodules are frequently detected at multidetector computed tomography (MDCT); in one screening MDCT study, most patients who underwent screening had at least one nodule (2). MDCT technology improves sensitivity and specificity for detecting pulmonary nodules by increasing spatial and contrast resolution and decreasing misregistration artifacts. The widespread use of MDCT has increased the

Table 1: Differential Diagnosis for Solid SPNs

Type of Cause	Condition
Neoplastic (malignant)	Primary lung malignancies (non–small cell, small cell, carcinoid, lymphoma), solitary metastasis
Benign	Hamartoma, arteriovenous malformation
Infectious	Granuloma, round pneumonia, abscess, septic embolus
Noninfectious	Amyloidoma, subpleural lymph nodule, rheumatoid nodule, Wegener granulomatosis, focal scarring, infarct
Congenital	Sequestration, bronchogenic cyst, bronchial atresia with mucoid impaction

Table 2: Differential Diagnosis for Persistent Subsolid SPNs

Type of Cause	Condition
Malignant	Lung adenocarcinoma (including preinvasive lesions, atypical adenomatous hyperplasia, and adenocarcinoma in situ); metastasis from melanoma, renal cell carcinoma, and adenocarcinoma of the pancreas, breast, and gastrointestinal tract*; lymphoproliferative disorders
Benign	Organizing pneumonia, focal interstitial fibrosis, endometriosis

*Source.—Reference 4.

detection of not only solid pulmonary nodules, but also subsolid nodules, and it provides more accurate characterization of nodules. **Subsolid nodules contain a component with ground-glass attenuation, which is higher than that of normal lung parenchyma and lower than that of soft tissue, such as the pulmonary vessels. Subsolid nodules may have purely ground-glass attenuation, be partly solid, or have mixed solid and ground-glass attenuation (3).**

The differential diagnosis for solid and subsolid SPNs is broad and includes benign causes as well as lung cancer (Tables 1, 2). The differential diagnosis for subsolid SPNs includes infection, inflammation, hemorrhage, and malignancy, specifically lung adenocarcinoma (5). The evaluation of SPNs, both solid and subsolid, is clinically important because they may be an early manifestation of lung cancer, the leading cause of cancer deaths in the United States (6). The American Cancer Society reports that one in 13 men and one in 16 women will be diagnosed with lung cancer and that approximately 20%–30% of those patients will present with an SPN (6,7).

Noninvasive imaging-based assessment and management of SPNs are evolving because of advances in MDCT technology, increased knowledge from lung cancer screening studies, and a better understanding of lung adenocarcinomas. Strategies for evaluating and managing solid and subsolid pulmonary nodules take into consideration nodule size; morphologic characteristics; growth rate; and patients' risk factors for malig-

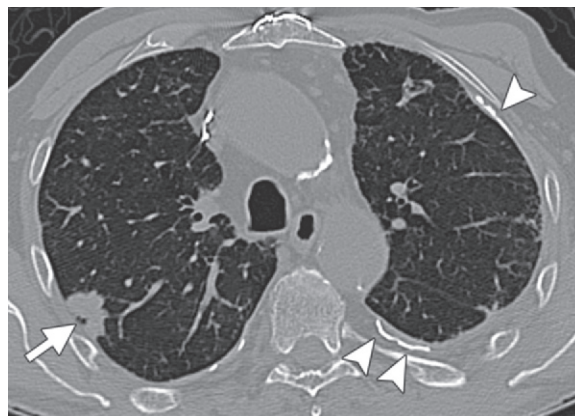
nancy, including age, smoking history, and history of malignancy, and require expertise across multiple disciplines, such as radiology, medical oncology, pulmonary medicine, cancer prevention, and thoracic surgery. Although subsolid nodules may demonstrate indolent behavior, it is important to identify the subset of lesions associated with invasive adenocarcinoma that necessitate more aggressive treatment. In this article, we discuss the role of imaging in evaluating solid and subsolid SPNs, imaging findings that help differentiate benign and malignant nodules, and treatment strategies and guidelines.

Clinical Evaluation

In the clinical management of SPNs, estimating the probability for malignancy is an important consideration. Factors associated with an increased risk for developing lung cancer include the patient's age; the presence of symptoms; a history of smoking; and a history of exposure to asbestos, uranium, or radon (Fig 1). For subsolid nodules, the Fleischner guidelines indicate that a history of smoking does not factor into the recommendations for management because there is an increasing incidence of lung adenocarcinoma in younger patients and those with no history of smoking. With regard to the initial clinical manifestation, there is an increased risk for malignancy in patients with hemoptysis and an SPN (8). Family history also plays a key role in determining the likelihood of malignancy. The risk for developing lung cancer increases in patients who

Teaching Point

Figure 1. Lung cancer in an 80-year-old man with a 45-pack-years smoking history and occupational exposure to asbestos. Unenhanced CT image of the chest shows a right upper lobe mass with a lobular contour (arrow) and calcified pleural plaques in the left hemithorax (arrowheads). In the clinical management of an SPN, estimating the probability for malignancy is important. Factors associated with an increased risk for developing lung cancer include advanced age, history of smoking, and exposure to asbestos.



have a first-degree relative with lung cancer (9). In terms of medical history, patients with a history of malignancy and pulmonary fibrosis have an increased risk for developing lung cancer (8). For patients with a history of cancer who underwent resection of small nodules, Ginsberg et al (10) reported that nodules 5 mm or smaller were malignant in 115 (42%) of 275 patients. Quantitative clinical prediction models have been developed to identify independent predictors of malignancy with the use of multiple logistic regression analysis. Independent predictors of malignancy include advanced age, a current or past smoking habit, and a history of extrathoracic cancer more than 5 years before detection of a nodule (11).

Radiographic Evaluation

Although many SPNs are depicted at CT, some are still initially seen at chest radiography. If a nodule is diffusely calcified or demonstrates a stable size for more than 2 years at comparison with prior radiographs, it has a high likelihood of being benign, and no further assessment is recommended. Technical innovations to improve the sensitivity of radiography for depicting nodules include dual-energy subtraction techniques and new bone-suppression software programs to decrease or completely remove overprojection of bones, mainly from the clavicles and ribs, which significantly hampers detection of pulmonary nodules (12). However, in many instances, nodules that are detected at radiography require further imaging evaluation.

Technique

MDCT is more sensitive than single-detector CT for depicting pulmonary nodules because of its higher contrast and spatial resolution. When thin sections are used, difficulty determining whether a small area of attenuation is a nodule, a vessel, or a result of partial-volume averaging of adjacent intrathoracic structures may be mitigated with postprocessing techniques, such

as maximum intensity projection, volume rendering, and cine viewing (13). Despite these advances, pulmonary nodules may still be missed at MDCT because of their small size, low attenuation (eg, ground-glass-attenuation nodules [GGANs]), perivascular central location, or adjacent parenchymal disease. MDCT plays a key role in evaluating morphologic characteristics and growth of nodules on serial images. **The use of thin sections minimizes partial volume effects and the resultant misinterpretation of a small solid nodule as a subsolid lesion, which may be managed differently, and enables three-dimensional analysis, including quantitative techniques.**

When performing MDCT for follow-up evaluation of nodules, attention to radiation dose is important. Low-dose techniques have been recommended for surveillance of lung nodules and typically use 120 kVp. A tube current of 40–80 mAs may be considered. It is important to be aware that, because of increased image noise, low-dose techniques may decrease the detection of faint ground-glass attenuation. Future investigation into iterative reconstruction will contribute to the understanding of any improvement in detecting GGANs with these newer reconstruction techniques. Dose savings may be achieved with the use of widely available tube current modulation techniques that serve as a form of automatic exposure control; the tube current is adjusted for overall patient size and varies, while CT data are acquired in the axial and longitudinal directions to maintain homogeneous image quality. Higher tube current is delivered to thicker and denser areas of the body, and lower tube current is delivered to the remaining areas. In general, CT data are reconstructed with a 512×512 matrix and a 25–35-cm field of view. Typical reconstructions consist of 2.5 mm and thicker sections for a nontargeted field of view. The use of thin sections (1.0–1.5 mm) in the region of interest improves z-axis spatial resolution and reduces partial-volume averaging, which

Teaching
Point

improves evaluation of small and subsolid nodules. Use of a high-frequency reconstruction algorithm maximizes the spatial resolution of margins and internal features of solid and subsolid nodules. Depiction of internal features is particularly important for evaluating subsolid nodules. In contrast, a low-frequency reconstruction algorithm, which minimizes image noise and decreases spatial resolution, is recommended for further evaluation of nodules that are suspected of containing fat or calcium (eg, hamartomas and granulomas). For this purpose, the use of a high-frequency algorithm may result in high-attenuation areas, which may lead to false identification of calcium within a nodule.

Solid Nodules

There is considerable overlap in the imaging characteristics of benign and malignant SPNs. However, specific morphologic features that are useful in determining the malignant potential of a nodule include size, margins, contour, internal characteristics (eg, attenuation, wall thickness in cavitary nodules, and air bronchograms), the presence of satellite nodules, the halo and reverse halo signs, and growth rate.

In terms of size, the likelihood of malignancy positively correlates with nodule diameter. As the diameter of a nodule increases, so does the likelihood of malignancy; however, a small nodule diameter does not exclude malignancy (14). Small nodules (<4 mm) have a less than 1% chance of being a primary lung cancer, even in people who smoke, whereas the risk for malignancy increases to 10%–20% for nodules in the range of 8 mm (14). This is particularly challenging because the widespread use of MDCT and the growing interest in lung cancer screening have resulted in frequent and incidental detection of small (1–5 mm) lung nodules (15). According to a review of eight CT lung cancer screening studies, the prevalence of SPNs ranges from 8% to 51%, and the prevalence of malignancy ranges from 1% to 12% (16).

In terms of nodule margins and contour, there is considerable overlap between benign and malignant lesions. Typically, benign nodules have well-defined margins and a smooth contour, whereas malignant nodules have spiculated margins and a lobular or irregular contour (8). Spiculation is attributed to growth of malignant cells along the pulmonary interstitium, whereas lobulation is attributed to differential growth rates within nodules (17). Specifically, a spiculated margin (which is often described as a sunburst or corona radiata sign) is highly predictive of malignancy, with a positive predictive value of 90% (18). However, benign conditions that result

from infection or inflammation, including lipoid pneumonia, focal atelectasis, tuberculoma, and progressive massive fibrosis, may also have a spiculated margin (19). In addition, a smooth margin does not exclude malignancy; many pulmonary metastases and as many as 20% of primary lung malignancies have smooth margins (20).

At CT, the halo sign—a poorly defined rim of ground-glass attenuation around the nodule—may represent hemorrhage, tumor infiltration, or perinodular inflammation (21). Originally described in invasive aspergillosis, the halo sign may also be seen with adenocarcinoma in situ (formerly known as bronchioloalveolar carcinoma); Kaposi sarcoma; and lung metastases from angiosarcoma, choriocarcinoma, and osteosarcoma (21). Conversely, the reverse halo sign (also known as the atoll sign), a central area of ground-glass attenuation surrounded by a halo or crescent of consolidation, was first described in cryptogenic organizing pneumonia and may be seen in patients with lung cancer after radiofrequency ablation (Fig 2) (22).

Fat attenuation (–40 to –120 HU) is characteristic of a hamartoma and is seen in as many as 50% of these neoplasms at CT (Fig 3) (23). Other causes of fat attenuation in an SPN include pulmonary metastases in patients with liposarcoma or renal cell cancer and lipoid pneumonia (24).

Calcification patterns may be useful in determining whether a nodule is benign, and CT is considerably more sensitive than radiography for depicting calcification (25). Thus, it is recommended that unenhanced CT be performed with thin sections (1–3 mm); a low-frequency, soft-tissue, or smooth reconstruction algorithm at the level of the nodule; and an attenuation value greater than 200 HU to determine whether calcifications are present within the nodule. Recently, with the introduction of dual-energy CT, in which 80- and 140-kV images are simultaneously obtained, measurement of CT attenuation values obtained at different kilovolt peaks may be used to identify areas of calcium and iodinated contrast material. A multicenter trial showed that the use of unenhanced dual-energy CT to evaluate changes in attenuation values at 140 and 80 kVp is not reliable for differentiating benign and malignant nodules with 3-mm sections and differing acquisitions for both kilovolt potentials (26). Common benign patterns of calcification include diffuse, central (a bull's-eye appearance), laminated, and popcorn. Diffuse, central, and laminated patterns are typically seen in granulomatous infections (Fig 4). Popcorn calcifications are characteristic of chondroid calcifications in hamartomas. However, it is important to be aware that lung metastases from chondrosarcomas or osteosarcomas may manifest

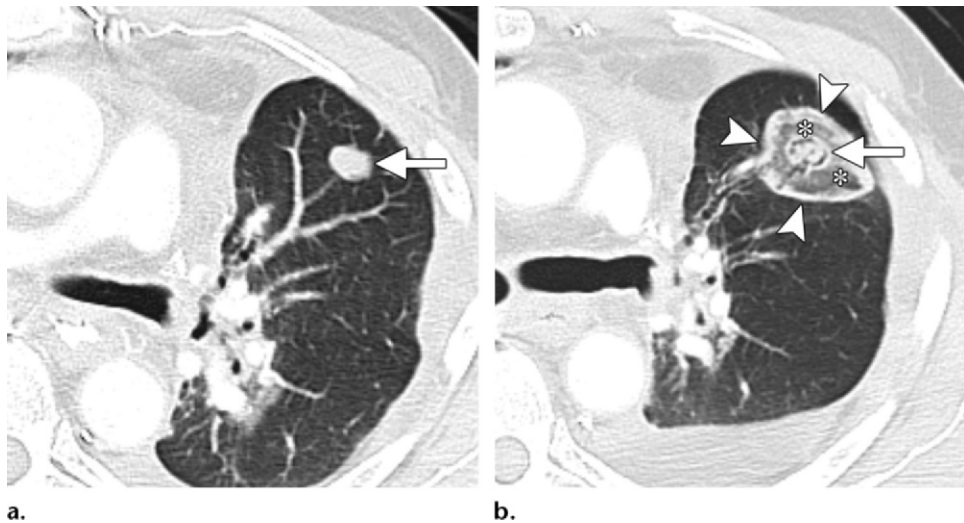


Figure 2. Reverse halo sign after radiofrequency ablation of a pulmonary metastasis in a 63-year-old man with pancreatic cancer who previously underwent left upper lobectomy. **(a)** Contrast-enhanced CT image shows a left-lower-lobe metastasis (arrow). **(b)** Contrast-enhanced CT image obtained 1 month after radiofrequency ablation shows the treated metastasis (arrow), which now has mixed attenuation, surrounded by a ground-glass opacity (*) and a well-circumscribed rim of consolidation (arrowheads), a finding known as the reverse halo sign. Originally described in cryptogenic organizing pneumonia, the reverse halo, or atoll, sign can also be seen in paracoccidioidomycosis, tuberculosis, lymphomatoid granulomatosis, Wegener granulomatosis, sarcoidosis, and tumors after radiofrequency ablation.

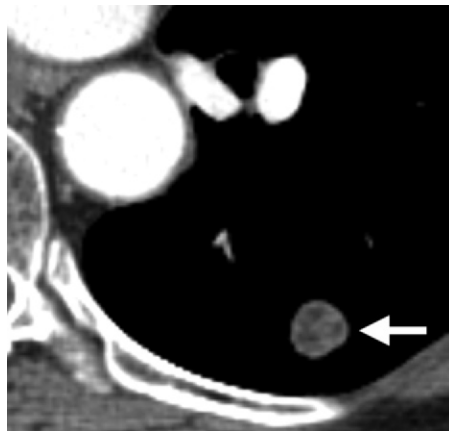


Figure 3. Hamartoma in a 72-year-old woman with an unknown primary malignancy that metastasized to the liver. Contrast-enhanced CT image shows a well-circumscribed left-lower-lobe nodule (arrow) with low attenuation (-46 HU), a finding consistent with fat. Focal fat can also be seen in a pulmonary nodule in liposarcoma metastases and lipid pneumonia.

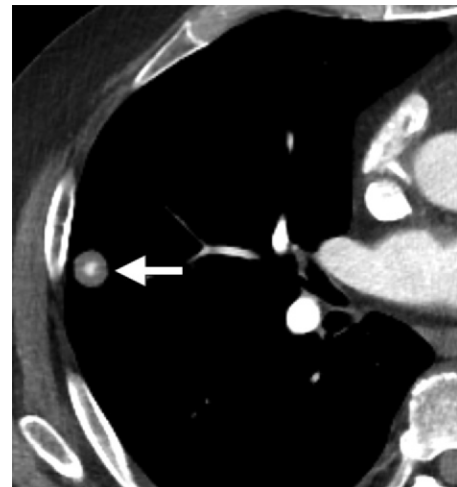


Figure 4. Benign pattern of calcification in granuloma in a patient from the Ohio River valley. CT image shows a central, or "bull's-eye," area of calcification (arrow) that is highly suggestive of granulomatous infection. The nodule is a result of *Histoplasma capsulatum* infection.

with these patterns of calcification and be misinterpreted as benign (27). Calcifications may be detected in 10% of all lung cancers at CT; indeterminate patterns include punctate, eccentric, and amorphous calcifications (28).

Cavitation occurs in both infectious and inflammatory conditions, such as abscesses, infectious granulomas, vasculitides, and pulmonary

infarctions, as well as malignancies such as primary and metastatic tumors, particularly those with squamous cell histologic characteristics. In terms of cavitary nodules, smooth, thin walls are typically seen in benign lesions, whereas thick, irregular walls are seen in malignant lesions. It has been reported that 95% of cavitary nodules with a wall thickness greater than 15 mm are

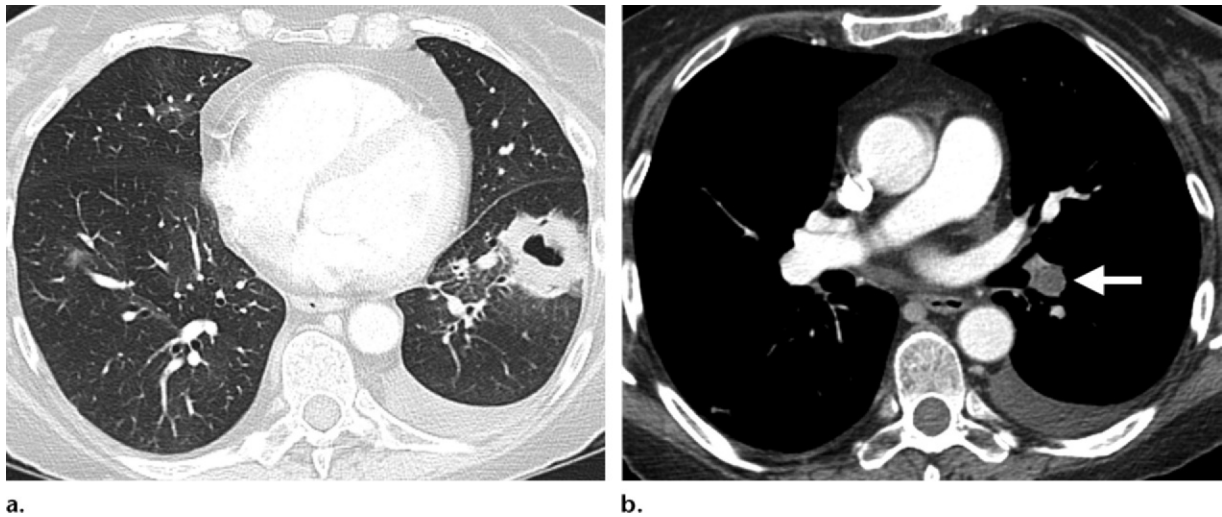


Figure 5. Pulmonary infarction mimicking malignancy in a 58-year-old woman with leukemia and deep venous thrombosis. **(a)** Contrast-enhanced CT image shows a thick-walled cavitary lesion in the left lower lobe and a small left pleural effusion. **(b)** Contrast-enhanced CT image shows a pulmonary embolism in the left interlobar pulmonary artery (arrow). Although cavitary wall thickness of more than 15 mm is typically seen in malignant lesions, knowledge of the clinical context is important to establish the diagnosis.

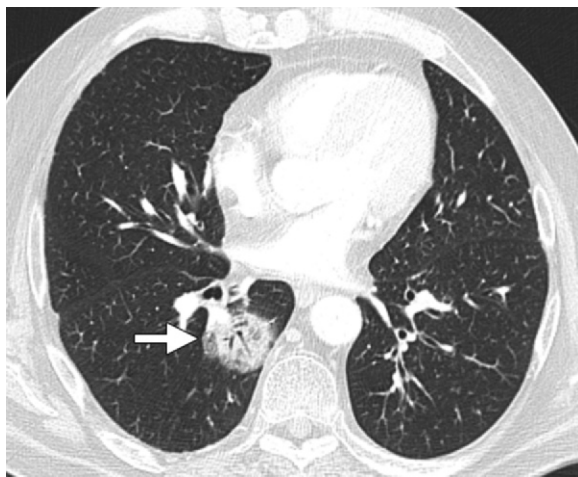


Figure 6. Fungal pneumonia and the air bronchogram sign in a 62-year-old man with leukemia 2 months after undergoing bone marrow transplantation. Contrast-enhanced CT image shows a right-lower-lobe lesion (arrow) and air-filled bronchi (the air bronchogram sign), findings consistent with pneumonia. Findings from fine needle aspiration biopsy confirmed *Aspergillus* infection. In addition to infection, the air bronchogram sign may be seen in patients with adenocarcinoma and lymphoma.

malignant, and 92% of cavitary nodules with a wall thickness less than 5 mm are benign (29). For cavities that were 5–15 mm in their thickest part, 51% were benign, and 49% were malignant. Thus, a cavity wall thickness of 5–15 mm may not be used to reliably differentiate benign and malignant nodules (Fig 5) (29). Bubbly lucencies may be seen within an SPN in patients with adenocarcinoma, lymphoma, sarcoidosis, or organizing pneumonia (30). Finally, lucencies within an SPN may be seen with the air bronchogram sign, which is defined as a pattern of air-filled bronchi against a background of airless lung and indicates patency of proximal airways and evacuation of alveolar air by means of absorption (atelectasis), replacement (eg, pneumonia), or both (31). The air bronchogram sign is reported to occur more frequently in malignant

nodules (29%) than in benign nodules (6%) and may be seen in patients with adenocarcinoma, lymphoma, or infection (Fig 6) (32).

Subsolid Nodules

Definition and Differential Diagnosis

Although the previously described morphologic features have been helpful in differentiating benign and malignant solid nodules, a new challenge in evaluating SPNs relates to subsolid nodules, which contain a portion of ground-glass attenuation that is higher than that of normal lung parenchyma and lower than that of soft tissue, such as blood vessels. Subsolid nodules may have purely ground-glass attenuation or be partly solid with areas of soft-tissue attenuation interspersed with areas of ground-glass attenuation (3,33). Subsolid nodules may result from infection, inflammation, hemorrhage, or neoplasm (5). Typically, inflammatory causes resolve at short-interval reassessment. Resolution and regression have been reported to occur in 37.6% of patients with

a GGAN and 48.7% of patients with a partly solid nodule (PSN) (34). Furthermore, after resection in patients with lung cancer, 174 GGANs developed during the period of observation (2.7 years), and 63% of them spontaneously resolved (35). Persistent subsolid nodules are more likely to be malignant, specifically primary lung adenocarcinoma, but they may also be benign (eg, focal interstitial fibrosis and organizing pneumonia) (36). In a study by Kim et al (36), 75% of persistent GGANs were adenocarcinoma, and 6% were atypical adenomatous hyperplasia.

Association with Adenocarcinoma

Adenocarcinoma, which constitutes approximately 50% of all lung cancers, is more likely to manifest as a solitary subsolid nodule (SSN) than other histologic subtypes of non-small cell lung cancer (37). Recently, a new taxonomy of adenocarcinoma was proposed to address many current issues and questions. The classification of lung adenocarcinoma by the International Association for the Study of Lung Cancer (IASLC), American Thoracic Society (ATS), and European Respiratory Society (ERS) includes a multidisciplinary approach that uses pathologic and imaging findings and molecular biology information (38). The IASLC, ATS, and ERS classification system uses clearer terminology to describe the degree of growth along the alveolar surface (ie, lepidic growth), and it uses invasive components to define preinvasive and invasive lesions (Fig 7) (33). Preinvasive lesions comprise atypical adenomatous hyperplasia (AAH) and adenocarcinoma in situ (AIS), both of which are defined as lesions that demonstrate lepidic growth (ie, they purely grow along the alveolar surface). Typically, AAH is a lesion with pure ground-glass attenuation that measures less than 1 cm, but larger lesions have been reported. AIS is typically a lesion with pure ground-glass attenuation that measures less than 3 cm and demonstrates pure lepidic growth without invasion. AAH and AIS are pathologic entities and are considered part of a spectrum; they may not be discriminated on the basis of cytologic findings. Note that the term *bronchioalveolar carcinoma (BAC)* is no longer used to enable more accurate pathologic discrimination among adenocarcinoma entities.

In the IASLC, ATS, and ERS classification of adenocarcinomas, invasive lesions include minimally invasive (MIA) and invasive adenocarcinoma. MIA is defined as a predominantly lepidic lesion that demonstrates no necrosis or invasion of lymphatics, blood vessels, or pleura; measures less than 3 cm; and has an invasive component that measures no more than 5 mm in any one location (33). MIA may be seen as a GGAN or

PSN at CT. Invasive adenocarcinoma is further classified on the basis of its histologic characteristics as having a predominantly lepidic, acinar, papillary, micropapillary, or solid pattern. For example, lepidic-predominant adenocarcinoma (LPA) has both mucinous and nonmucinous forms. The more common nonmucinous form of LPA is defined as a lepidic lesion that may have necrosis, invade lymphatics or blood vessels, and have a focus of invasion larger than 5 mm. Similarly, AIS and MIA also have both mucinous and nonmucinous forms. For mucinous malignancies, invasive mucinous adenocarcinoma has replaced the term *mucinous BAC* and typically manifests as a solid nodule or an area of consolidative attenuation.

CT Technique

Detecting SSNs at CT can be challenging given their low contrast relative to the surrounding lung parenchyma and their poorly defined margins. However, increasing awareness of SSNs and improvements in multidetector CT technology has resulted in improved detection. In the evaluation of subsolid nodules, the use of postprocessing techniques and computer-aided diagnosis (CAD) has been investigated to improve depiction of nodules (39). The minimal-intensity-projection technique, in which the lowest voxel along an array within a section is selected, minimizes the appearance of vasculature and improves the visibility of GGANs (39). The use of CAD has been shown to improve detection of GGANs (40). Obtaining thin-section volumetric CT data facilitates evaluation of subsolid lesions in three dimensions and, therefore, minimizes misinterpretation of findings that mimic nodules. For example, reconstructing images in an additional plane (eg, the coronal plane) enables assessment of the craniocaudal dimension and helps differentiate linear scarring or atelectasis from true subsolid nodules. Similarly, the use of thin sections helps avoid misinterpreting volume averaging from parenchymal, mediastinal, and chest wall structures as true subsolid nodules.

CT Findings and Morphologic Characteristics

After an SSN is initially detected, reassessing with CT at 3 months is important to determine its persistence, because lesions that result from infectious or noninfectious inflammatory causes may regress or resolve in the interval (Fig 8). For persistent SSNs, CT features, including nodule attenuation and the presence and size of any solid component, are important for differentiating benign from malignant nodules. In terms of the IASLC, ERS, and ATS classification, adenocarcinomas have both

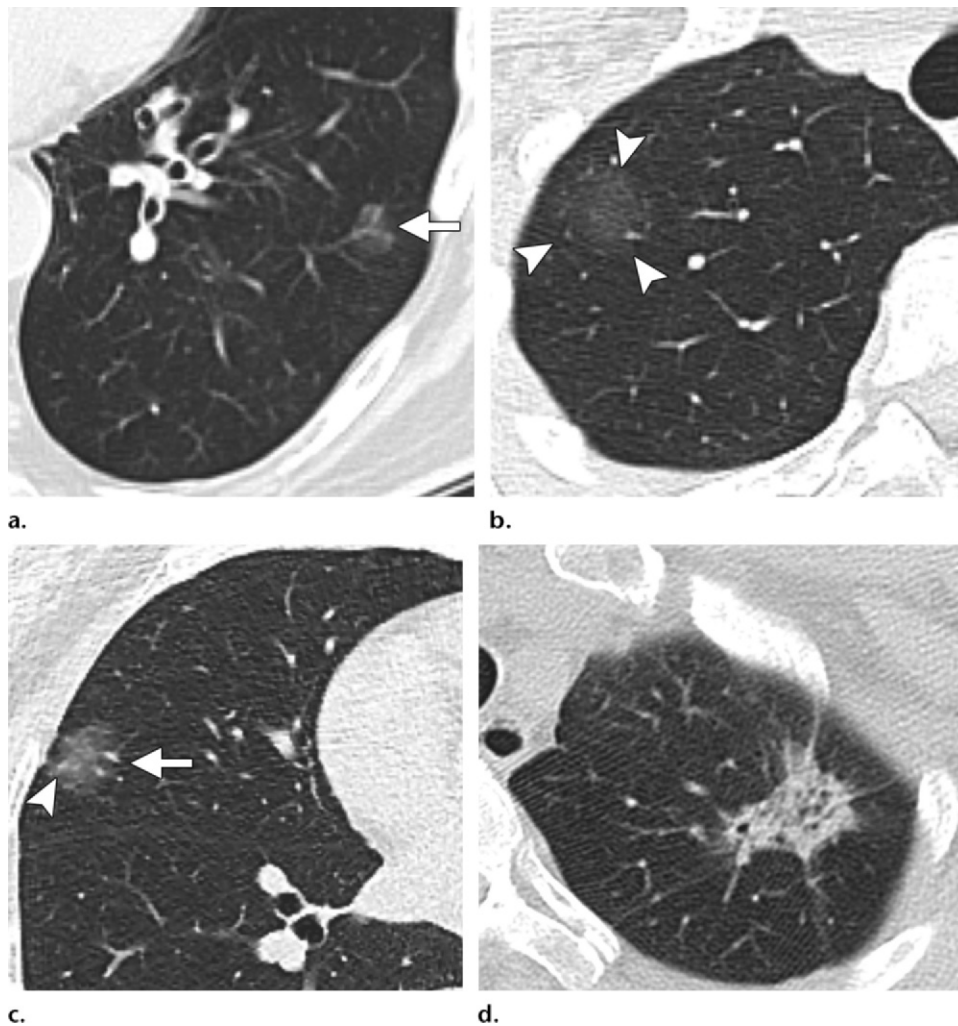


Figure 7. IASLC, ATS, and ERS classification of lung adenocarcinoma, in which preinvasive lesions include atypical adenomatous hyperplasia (AAH) and adenocarcinoma in situ (AIS), both of which are defined as lesions with purely lepidic growth along the alveolar surface. **(a)** CT image shows an AAH lesion (arrow), which typically has pure ground-glass attenuation and measures less than 1 cm. However, lesions larger than 1 cm have been reported. **(b)** CT image shows an AIS lesion (arrowheads), which typically has pure ground-glass attenuation and measures less than 3 cm. Invasive lesions include minimally invasive adenocarcinoma (MIA) and invasive adenocarcinoma, which are further classified as having a lepidic, acinar, papillary, micropapillary, or solid-predominant pattern. **(c)** CT image shows an MIA lesion (arrow), which has a predominantly lepidic pattern; lacks necrosis; does not invade lymphatics, blood vessels, or pleura; measures less than 3 cm; and has an invasive component (arrowhead) that measures no more than 5 mm in any one location. **(d)** CT image shows a lepidic-predominant adenocarcinoma (LPA) in its nonmucinous form. Necrosis may be present, and the focus of invasion of lymphatics and blood vessels is greater than 5 mm.

mucinous and nonmucinous forms. Correlation of CT and histopathologic findings with the IASLC, ERS, and ATS system is still evolving, and studies that describe CT manifestations of subsolid nodules mostly pertain to the nonmucinous forms and are summarized in the next paragraph. In contrast, the less common mucinous form of AIS, MIA, LPA, and other forms of invasive adenocarcinomas may manifest as a solid nodule.

Typically, nonmucinous forms of AAH and AIS manifest as a pure GGAN at CT (Table 3).

AAH has primarily been described as a small round or oval GGAN with smooth, well-defined borders (41). It is typically 5 mm or smaller, but nodules larger than 10 mm have been reported (38,42). Typically, AIS has pure ground-glass attenuation and is less than 3 cm, but may occasionally demonstrate partly solid attenuation. Differentiating AAH and AIS is not possible at CT (42). The appearance of nonmucinous forms of invasive adenocarcinomas (eg, MIA and LPA) at CT varies. MIA may manifest as a PSN that is

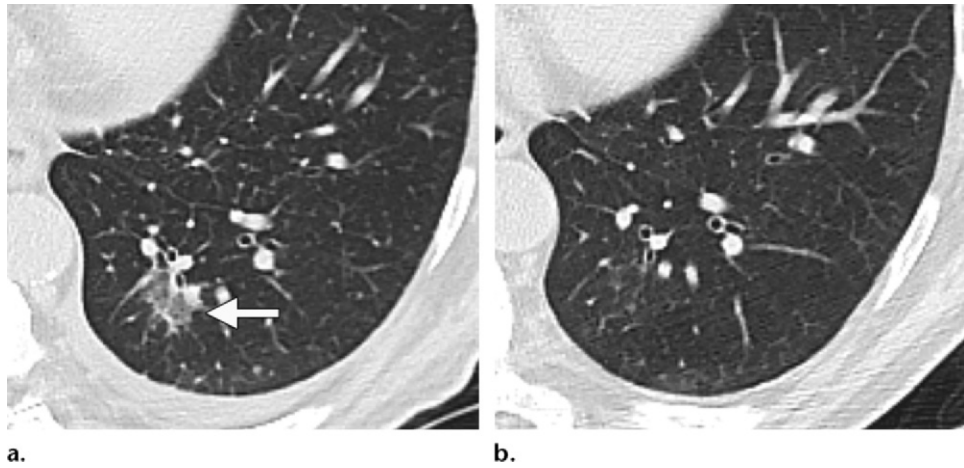


Figure 8. GGAN resulting from infection in a 66-year-old man with leukemia who presented with fever. **(a)** Coned-down CT image shows a ground-glass opacity (arrow) in the left lower lobe. **(b)** Follow-up CT image obtained 3 months later shows resolution of the ground-glass opacity. For subsolid lesions, initial follow-up CT is performed at 3 months to determine persistence, because lesions that result from infectious or inflammatory causes may regress or resolve in the interval.

Table 3: Classification of Nonmucinous Forms of Lung Adenocarcinoma and CT Features of Subsolid Nodules

2011 IASLC, ATS, and ERS Classification	CT Features
Atypical adenomatous hyperplasia	GGAN
Adenocarcinoma in situ	GGAN with a possible solid component
Minimally invasive adenocarcinoma	GGAN, partly solid nodule
Lepidic-predominant adenocarcinoma	Partly solid nodule, solid nodule
Invasive adenocarcinoma classified by predominant subtype	Partly solid nodule with a solid component, solid nodule

less than 3 cm with predominantly ground-glass attenuation and an invasive component of 5 mm or more in any one location. LPA may manifest as a PSN with necrosis and a focus of invasion of lymphatics or blood vessels greater than 5 mm. In terms of CT characterization of PSNs, a central location of the solid component is seen more often in malignant lesions (43). The soft-tissue component of subsolid nodules may represent an invasive component and/or fibrosis with alveolar collapse. Currently, the degree of invasion is reported to directly correlate with the size of the soft-tissue component at CT (Table 3) (38,44,45).

Various methods have been investigated to improve characterization of the degree of invasion of subsolid adenocarcinomas. Yamada et al (46) measured the CT attenuation values of the solid part of subsolid nodules and compared them with pathologic features (46). The authors reported that attenuation was significantly higher in the group with invasion compared with that in groups with no or micro invasion. Ikeda et al (47) reported that the mean nodule attenuation number could

be used to differentiate among AAH (−609 HU), BAC (−450 HU), and invasive adenocarcinomas (−319 HU). The proportion of the solid component to the ground-glass component has also been proposed as a feature to characterize PSNs in terms of aggressiveness (48). Suzuki et al (49) characterized the presence and distribution of soft tissue within 349 stage I adenocarcinomas that were 2 cm or less in size. The tumors ranged from pure GGANs to PSNs to solid lesions at CT. A direct correlation was reported between increasing attenuation and the presence and size of a solid component in an SSN with the degree of invasion of adenocarcinomas. Specific quantitative measures to express the ratio of the solid-to-ground-glass attenuation portions, such as a nodule disappearance ratio and the percentage of the solid component, have been investigated (48). Honda et al (45) reported that a ratio of the largest tumor dimension on images obtained with soft-tissue window settings versus that on images obtained with lung window settings of 50% or less indicated an “air-containing type,” and a ratio of more than

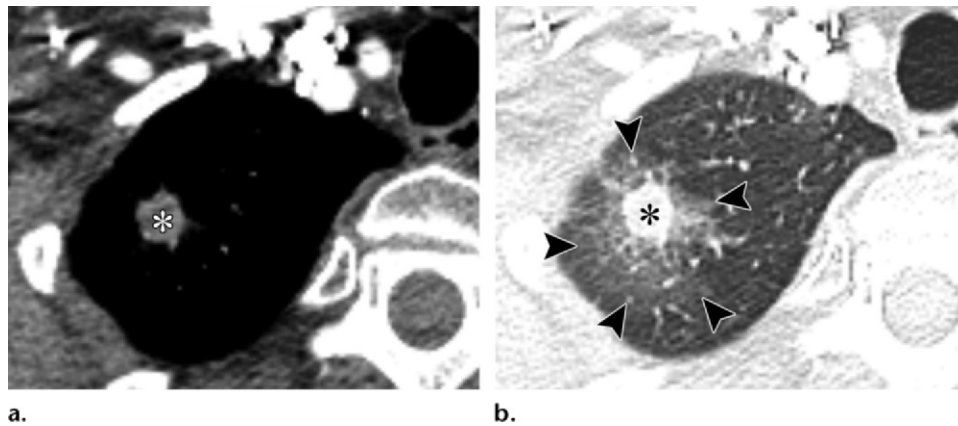


Figure 9. Fleischner Society recommendations for measuring subsolid lesions at CT. **(a)** CT image obtained with narrow and/or mediastinal window settings shows the solid component (*) of a subsolid lesion. **(b)** CT image obtained with wide and/or lung window settings shows the ground-glass-attenuation component (arrowheads) of the lesion. Measurements are based on the average of the long and short axis dimensions. Determination of the percentage of solid to ground-glass-attenuation components is important, because the greater the solid component, the more likely that the lesion is an invasive adenocarcinoma. * = solid component.

50% indicated a “solid type” lesion. They also reported that 114 of 142 air-containing lesions were AIS, whereas none were invasive adenocarcinomas. In contrast, 30 of the 158 solid-type lesions were AIS, 24 were MIA, and 104 were invasive adenocarcinomas (45). Although there is currently no standard CT methodology for quantifying the soft-tissue component of SSNs, direct correlation of the soft-tissue component with the degree of invasion or aggressiveness of subsolid adenocarcinomas and patient prognosis and survival has been reported (Fig 9) (50).

Other Morphologic Features

The morphologic features of nodule attenuation and the presence of a solid component are important in the evaluation of subsolid lesions. Other morphologic features have variable utility in differentiating benign from malignant lesions. In an evaluation of subsolid nodules, Kim et al (36) reported that there are no imaging features that may be used to reliably differentiate inflammatory and malignant entities. For subsolid nodules, size is of limited use in determining malignancy. Although AAHs are typically GGANs that are 5 mm or smaller, they may be larger than 1 cm (38). GGANs that are larger than 1 cm may be benign or malignant. In a study of resected persistent GGANs, it was reported that AAH had a mean diameter of 8 mm, adenocarcinoma (formerly BAC) had a mean diameter of 13 mm, and fibrosis (or organizing pneumonia) had a mean diameter of 12 mm (36,51). In terms of shape, Li et al (43) reported that a round shape is more common in malignant subsolid nodules (65%) than it is in benign modules (17%). In

contrast, Oda et al (52) reported that a round shape indicates AAH rather than adenocarcinoma. The presence of notches in the nodule margin and pleural tags are more frequent in invasive adenocarcinoma compared with MIA and AIS (45). In addition, lobulation, spiculation, a well-defined but coarse interface, and pseudocavitation (a bubbly appearance) have been reported to occur much more frequently in malignant subsolid lesions than they do in benign lesions (53). In malignant lesions, the presence of pseudocavitation results from sparing of alveoli or bronchi by tumor infiltration (54). However, there is considerable overlap of findings, because infectious and inflammatory causes may also demonstrate pseudocavitation. In patients who are immunocompetent, nodules that exhibit both pseudocavitation and the halo sign are reported to have a high likelihood of being adenocarcinoma (55). Future investigation into computer-aided techniques may enable internal features of nodules to be evaluated. For example, Kim et al (56) provided a CAD algorithm to detect and evaluate GGANs on the basis of texture features, including kurtosis, surface curvature, and three gray-level co-occurrence matrix features (inertia, maximum probability, and momentum) that improved detection of malignant GGANs.

Assessment of Malignant Potential

Nodule Growth

When assessing the malignant potential of solid and subsolid SPNs, growth is important to differentiate benign and malignant lesions. Typically, nodule growth is assessed on the basis of volume

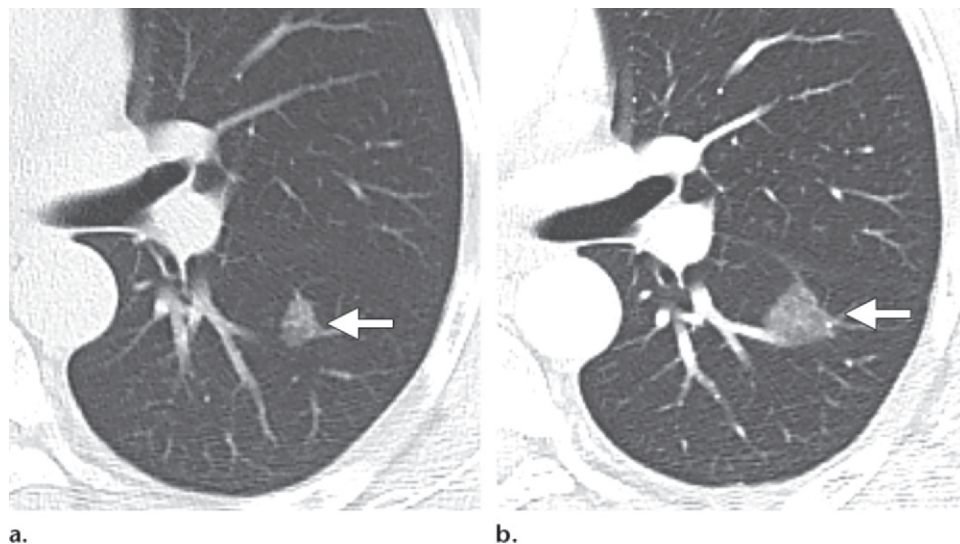


Figure 10. Subsolid lesion that increased in size, which indicates an increased risk for malignancy, in a 55-year-old man. **(a)** Coned-down contrast-enhanced CT image shows a 1.3-cm nodule (arrow) with pure ground-glass attenuation in the left lower lobe. Pulmonary vessels are visible within the lesion. The Fleischner Society recommends that solitary pure GGANs larger than 5 mm undergo initial follow-up CT in 3 months to determine persistence followed by yearly surveillance CT for a minimum of 3 years if the nodule is persistent and remains unchanged. This lesion persisted at 3-month follow-up CT. **(b)** Follow-up CT image obtained 3 years later shows the lesion, which increased in size to 1.8 cm. Biopsy was performed, and results of histologic analysis revealed adenocarcinoma. Because the volume-doubling time of subsolid lung cancers is typically longer than that for lung cancers that manifest as a solid nodule, imaging reassessment is recommended for an extended period of time for patients with a subsolid nodule.

doubling time; because nodules are usually spherical, nodule volume is calculated with the equation $4\pi r^3$. A doubling in volume manifests as a 26% increase in diameter. Malignant solid SPNs usually have a volume doubling time of less than 100 days, with a range of 20–400 days (54). Typically, nodules with a volume doubling time of less than 20 days have an infectious or inflammatory cause, whereas those with a volume doubling time of more than 400 days are usually benign (58). This growth characteristic does not apply to subsolid adenocarcinomas, which may take up to 1346 days to double in volume (59). **In terms of the range of volume doubling times for adenocarcinomas, tumors that manifest as a GGAN have a greater volume doubling time than do those that manifest as a PSN, which, in turn, have a greater volume doubling time than do solid lesions (60).**

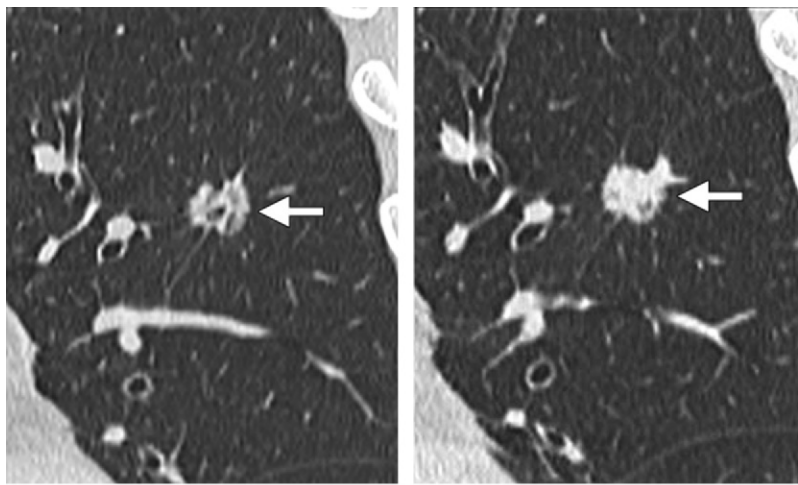
For solid nodules, it is generally accepted that a stable size over a 2-year period (which indicates a doubling time greater than 730 days) is a reliable determinant of benignity (61). However, for small nodules that double in volume, a change in diameter is difficult to perceive. Thus, concern has been raised about the accuracy of conferring benignity to small nodules on the basis of an absence of growth over 2 years. For subsolid nodules, the limitations in assessing growth are

compounded because these lesions are typically small and poorly defined with growth that may be indolent and difficult to perceive (62). **In contrast to growth in solid nodules, which is based solely on size, in subsolid nodules, growth may manifest as an increase in size, an increase in attenuation, development of a solid component, or an increase in size of a solid component. In subsolid nodules, these imaging features of growth indicate an increased risk for malignancy (Figs 10–12).** Kakinuma et al (63) reported that at follow-up imaging, adenocarcinomas that manifested as a subsolid lesion demonstrated an increase in size, an increase in attenuation, and development of a solid component. Scrutiny of the spatial relationship of the subsolid lesion with adjacent anatomic landmarks and the soft-tissue component with the ground-glass-attenuation component may help detect subtle interval growth.

It has been suggested that the use of three-dimensional volumetric assessment, rather than diameter, is a more accurate and reproducible method for determining the size and growth of solid and subsolid SPNs (64). However, there is considerable controversy regarding the most accurate method for assessing the growth rate of solid and subsolid nodules. Recently, mass, which is defined as the combination of nodule volume

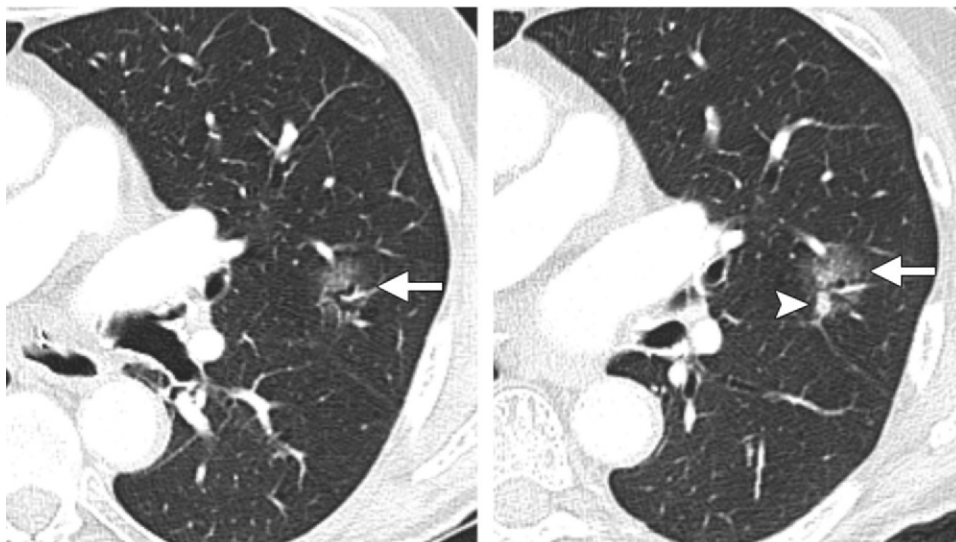
Teaching
Point

Teaching
Point



11a.

11b.



12a.

12b.

Figures 11, 12. (11) Increased attenuation in a subsolid lesion, which indicates an increased risk for malignancy. (a) Coned-down CT image of the chest with coronal reformation shows a 1.2-cm subsolid nodule (arrow) in the left upper lobe. (b) Follow-up CT image obtained 1 year later shows the nodule (arrow), which demonstrates increased attenuation, in addition to an increase in the overall size. According to the American College of Chest Physicians (ACCP) algorithm, an increase in nodule attenuation should be interpreted as an indicator of possible malignancy, and, in most cases, surgical resection should be strongly considered. (12) Development of a soft-tissue component in a subsolid lesion, which indicates an increased risk for malignancy, in an 85-year-old man with a history of adenocarcinoma that was treated with right upper lobectomy. (a) Contrast-enhanced CT image shows a 1.8-cm nodule with pure ground-glass attenuation (arrow) in the left upper lobe. Pulmonary vessels and the air bronchogram sign are visible in the lesion. (b) Follow-up CT image obtained 3 months later shows the nodule (arrow), with a new solid component posteriorly (arrowhead). Biopsy was performed, and results of histologic analysis revealed adenocarcinoma. A direct correlation between the soft-tissue component and the degree of invasion or aggressiveness of subsolid adenocarcinomas and patient prognosis and survival has been reported.

and density, was proposed as a more accurate determinant of growth of subsolid nodules. CT data may be used to calculate mass because x-ray attenuation values are proportional to tissue density (ie, mass per unit volume) (65). By multiplying nodule volume and density, mass measurements allow growth of SSNs to be detected ear-

lier and are subject to less variability than volume or diameter measurements (65).

It is important to be aware of two unusual patterns of growth of lung cancers that are potential pitfalls in interpretation. The finding of an isolated cystic airspace with increased wall thickness should raise the suspicion of lung cancer (Fig 13).



a.

b.

Figure 13. Lung cancer manifesting with increased wall thickness of a cystic airspace in a 77-year-old man with a history of right upper lobectomy for adenocarcinoma. **(a)** Contrast-enhanced CT image shows a cystic airspace (*) in the right lower lobe. **(b)** Follow-up CT image obtained 6 months later shows a new soft-tissue component (arrows) along the wall of the cystic airspace. Results of histologic analysis of the soft-tissue component revealed adenocarcinoma. The finding of an isolated cystic airspace with increased wall thickness should raise the suspicion for lung cancer.



a.

b.

c.

Figure 14. Transient decrease in size of a lung cancer. **(a)** CT image obtained at the patient's initial presentation shows a nodule (arrow) in the left lower lobe. **(b)** Follow-up CT image obtained 1 year later shows the nodule (arrow), which decreased in size. **(c)** CT image obtained 2 years after the initial presentation shows the nodule (arrow), which increased in size and lobularity. Although most lung cancers grow at a steady rate, temporary regression and growth can occur. It is postulated that a transient decrease in size may be related to the development of a fibrous component and/or collapse of fibrosis. Accordingly, a decrease in size requires continued imaging reassessment to confirm long-term stability or resolution.

The increased thickness of the wall may be solid or have ground-glass attenuation. In a study by Farooqi et al (66), 26 lung cancers were identified abutting the wall or in the wall of a cystic airspace. Histologic analysis showed that the cystic space resulted from a bulla, a fibrous-walled cyst, or a pleural bleb, and the wall of the airspace was unevenly thickened (66). Another potential pitfall relates to temporary regression of SPNs (Fig 14). Although most lung cancers grow at a steady exponential rate, a temporary regression in growth can occur (67). In a small study, Lindell et al (67) reported that 11 out of 18 cancers showed a decrease in volume at some point on their growth

curves. It is postulated that a transient decrease in size may be related to the development of a fibrous component and subsequent collapse of the fibrosis. Accordingly, a decrease in nodule size requires continued imaging reassessment to confirm long-term stability or resolution.

Nodule Enhancement

For solid SPNs, nodule enhancement can be quantitatively assessed at CT to differentiate benign and malignant lesions. In a multi-institutional trial, contrast material-enhanced CT was shown to be useful in determining the risk for malignancy of nodules as small as 5 mm (68). The degree of

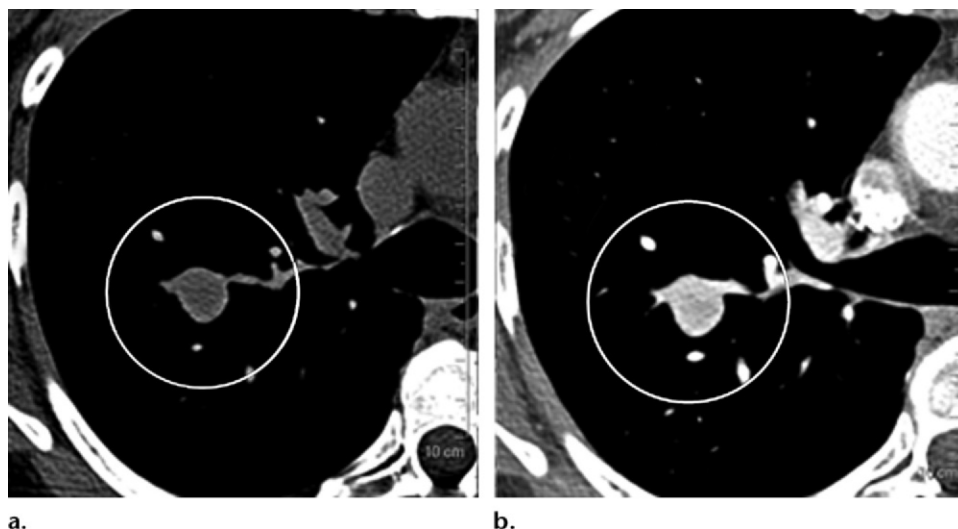


Figure 15. CT enhancement study in a 54-year-old woman with endometrial hyperplasia. CT images obtained before (**a**) and after (**b**) administration of intravenous contrast material show the nodule has enhanced, with an increase in attenuation values of 109 HU. Typically, malignant nodules enhance with an increase in attenuation values of more than 20 HU, whereas benign nodules enhance with an increase in attenuation values of less than 15 HU. Results from transthoracic needle aspiration biopsy revealed carcinoid tumor.

nodule enhancement correlates with the degree of vascularity, which increases in malignant lesions (68). The CT enhancement protocol comprises 3-mm collimation images of the nodule obtained before and after intravenous administration of contrast media. Serial 5-second spiral images are acquired at 1, 2, 3, and 4 minutes after the onset of contrast material administration. Enhancement is determined by subtracting the precontrast attenuation of the nodule from the peak attenuation after administration of contrast material. Measurement of the circular or oval region of interest (ROI) is made with mediastinal window settings to minimize partial volume averaging, with the ROI centered on the image closest to the nodule equator and comprising roughly 70% of the nodule diameter. Typically, malignant nodules enhance more than 20 HU, whereas benign nodules enhance less than 15 HU (Fig 15) (68). Nodules that enhance less than 15 HU are almost certainly benign (negative predictive value, 96%; sensitivity, 98%; specificity, 58%; accuracy, 77%) (68). It is important to note the limitations of this technique. It may be prudent to use this enhancement technique for nodules with a diameter of 2 cm or less, because smaller nodules have a higher likelihood of benignity and are less likely to have substantial necrosis. CT enhancement should be calculated only in nodules with a relatively spherical shape and homogeneous attenuation (ie, no evidence of fat, calcification, cavitation, or necrosis).

Recently, CAD has been used to evaluate vascular enhancement and morphologic characteristics to differentiate between benign and malignant

nodules. In a study by Shah et al (69), quantitative features, such as size, shape, attenuation, and enhancement properties, were used to differentiate between benign and malignant nodules and showed that, with the use of volumetric and contrast-enhanced data from 35 CT data sets of SPNs with a mean diameter of 25 mm (range, 6–54 mm), CAD helps differentiate between benign and malignant SPNs.

Nodule Metabolism

Functional imaging with fluorine 18 (^{18}F)-labeled fluorodeoxyglucose (FDG) positron emission tomography (PET) is a more widely used alternative to measuring nodule enhancement in the evaluation of solid SPNs. FDG is a measure of glucose metabolism and is used to differentiate between benign and malignant nodules. The most common semiquantitative method for evaluating pulmonary lesions at PET is the FDG standardized uptake value (SUV). Typically, metabolism of glucose is increased in malignancies, and, historically, an SUV cutoff of 2.5 has been used to differentiate between benign and malignant nodules, although visual analysis is just as accurate (70). PET has sensitivity and specificity of approximately 90% for detecting malignant nodules with a diameter of 10 mm or larger (71). Determination of the utility of FDG PET for evaluating SPNs takes into consideration clinical risk factors—such as a patient's age, smoking history, and history of malignancy—and imaging features to determine a management course. For example, in a

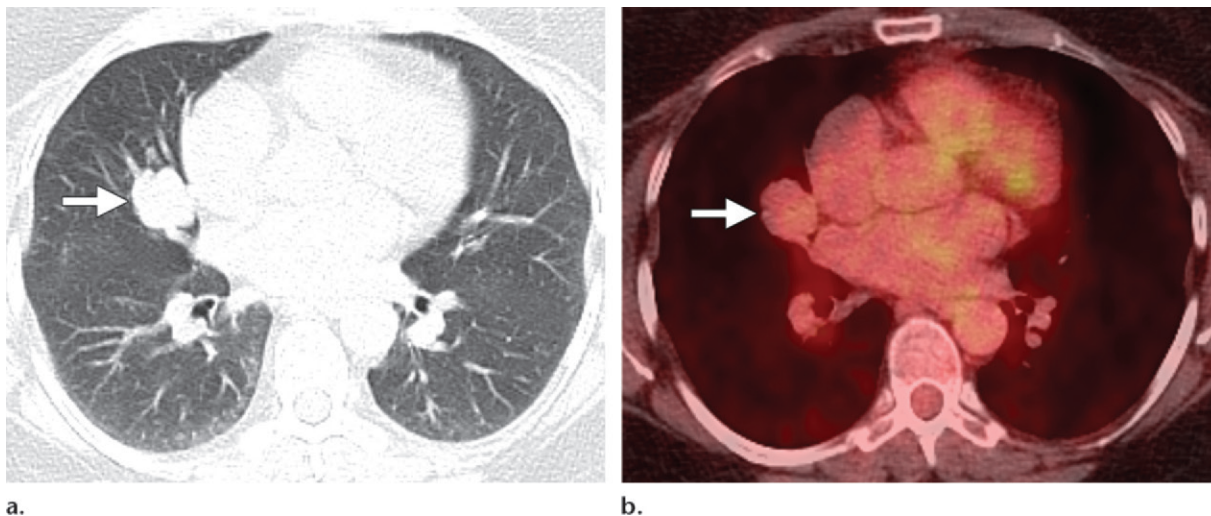


Figure 16. PET-negative neuroendocrine tumor in a 59-year-old woman. Unenhanced CT (a) and PET/CT (b) images show a well-circumscribed nodule in the middle lobe (arrow) with no FDG uptake. Results from transthoracic needle biopsy revealed a well-differentiated neuroendocrine tumor (carcinoid). False-negative PET findings can also occur in patients with indolent adenocarcinomas.

patient with a low pretest likelihood (20%) of malignancy who is being considered for serial imaging reassessment, negative findings at PET reduce the likelihood of malignancy to 1%, favoring conservative management (72). However, in a patient with a high pretest likelihood (80%) of malignancy, negative findings at PET only reduce the likelihood of malignancy to 14%; thus, a more aggressive course of action may be considered, such as obtaining tissue for biopsy or resection (72).

It is important to note that the high sensitivity and specificity of PET for evaluating SPNs pertains to solid nodules with a diameter of 10 mm or more. In contrast, FDG uptake in malignant GGANs and PSNs varies and cannot be used to reliably distinguish among benign and malignant lesions. In a recent study, nine out of 10 well-differentiated adenocarcinomas that manifested as a nodular ground-glass opacity were falsely negative at PET, whereas four out of five benign nodular ground-glass opacities were falsely positive (73). In this study, the sensitivity (10%) and specificity (20%) of PET for evaluating ground-glass opacities were significantly lower than those for evaluating solid nodules (90% and 71%, respectively).

In addition to its limitations for evaluating subsolid lesions, PET also has limited spatial resolution, which may lead to false-negative findings when lesions smaller than 10 mm in diameter are assessed (73,74). Today, evaluation of nodules approximately 7 mm in diameter is possible with commercially available PET scanners. Finally, false-negative PET findings are uncommon but may occur with carcinoid tumors and adenocar-

cinomas (Figs 16, 17) (75). The lower positive predictive value of PET in evaluating SPNs relates to the false-positive results that result from infection and inflammation (Figs 18, 19).

The introduction of integrated PET/CT scanners has enabled the near-simultaneous acquisition of coregistered, spatially matched functional and anatomic data sets. The temporal and spatial integration of these two data sets may be useful when PET/CT is the initial imaging modality in an SPN evaluation (76). In a study comparing PET/CT and helical dynamic CT (HDCT) for the evaluation of SPNs, PET/CT was more sensitive (96% vs 81%) and more accurate (93% vs 85%) than HDCT (76). However, the use of CT for attenuation correction of the PET images introduced artifacts and quantitative errors and can lead to misinterpretation of findings. For example, acquiring images during different stages of the patient's respiratory cycle may introduce a mismatch between the CT attenuation data obtained during breath holding and the PET data obtained during quiet tidal breathing (77). In addition to localization errors, this misregistration may also result in incorrect attenuation coefficients applied to the PET data, which may affect SUV, the most widely used parameter to quantify the intensity of FDG uptake (77). Misregistration may lead to an underestimation of the SUV and potentially result in false-negative results. Strategies to mitigate the respiratory mismatch between CT and PET images include acquiring CT images mid expiration, which most closely approximates the lung volumes at quiet tidal breathing, when PET images are acquired. However, acquiring

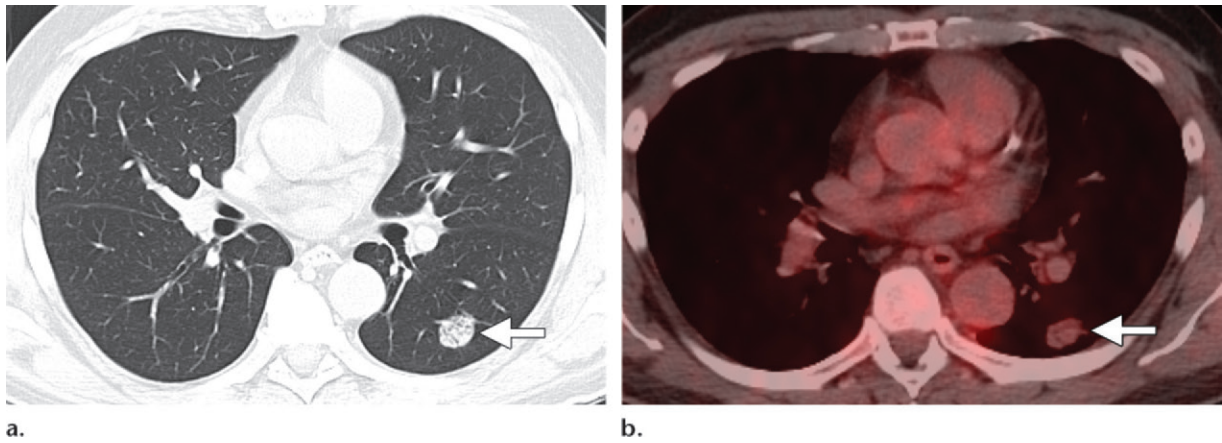


Figure 17. Decision analysis for a subsolid lesion in a 57-year-old man with thyroid and prostate cancer. **(a)** Unenhanced CT image of the chest shows a 1.5-cm subsolid lesion (arrowheads) in the left lower lobe with internal bubbly areas of attenuation and a soft-tissue component larger than 5 mm. The lesion persisted at 3-month follow-up CT. According to the Fleischner Society recommendations, a solitary PSN with a solid component that is larger than 5 mm should be considered malignant until proved otherwise. **(b)** PET/CT image obtained for preoperative staging shows no FDG uptake within the nodule (arrow). There was no evidence of nodal or metastatic disease at PET/CT. Negative PET findings do not preclude malignancy. Because of the high clinical suspicion for malignancy, transthoracic needle aspiration biopsy was performed, and adenocarcinoma was revealed.

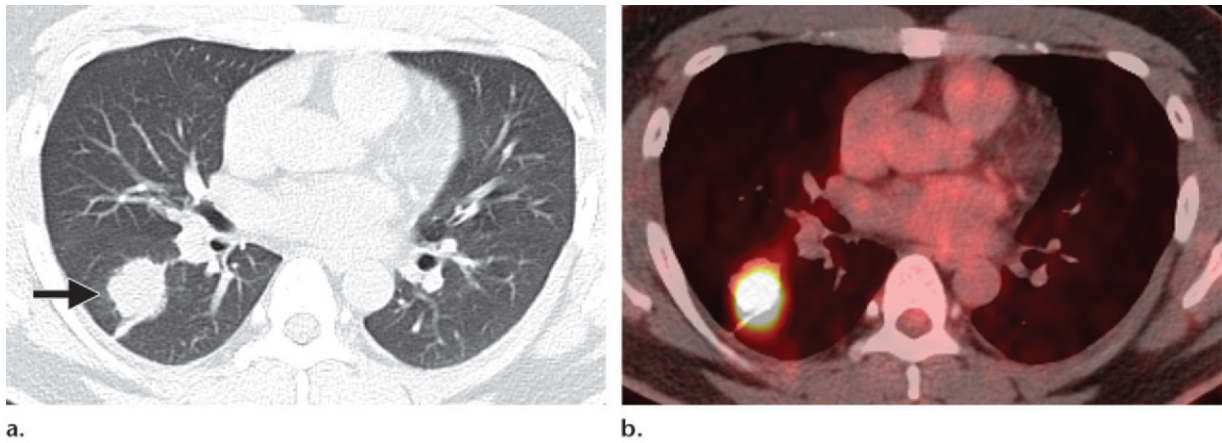
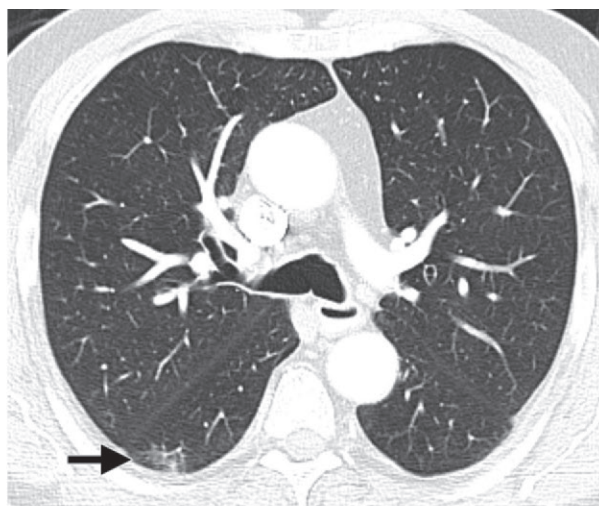


Figure 18. Infection mimicking malignancy in a 30-year-old man with no symptoms and a right lower lobe mass detected at chest radiography performed for a routine occupational health examination. **(a, b)** Unenhanced CT **(a)** and PET/CT **(b)** images show a 3-cm solid lesion in the right lower lobe (arrow in **a**) with a maximum SUV of 16.7. Biopsy results revealed granulomatous inflammation and no malignant cells. **(c)** Follow-up CT image obtained 2 months later shows regression of the lesion (arrow). Infectious and inflammatory conditions can accumulate FDG and be misinterpreted as malignant.

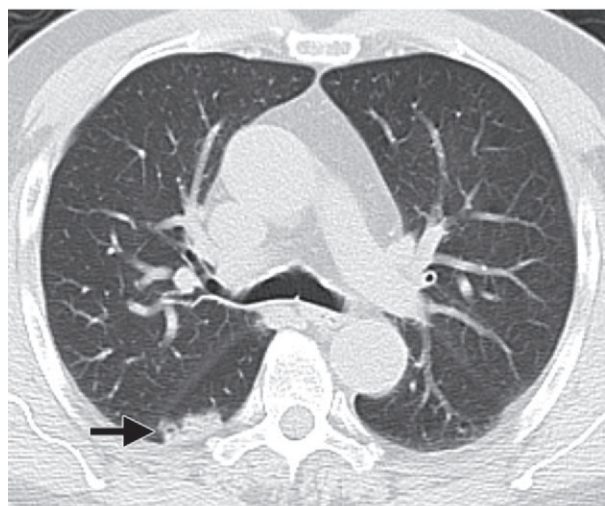
CT images of the lungs at mid expiration compromises anatomic detail, and small nodules in the lung bases may be missed. A more recent approach suggests the use of respiratory-averaged CT (CT cine images obtained over differ-

ent portions of the respiratory cycle with four-dimensional CT techniques) to improve SUV quantification (78). Respiratory-averaged CT used for PET attenuation correction has shown maximum SUV differences of more than 50% in some lesions, compared with the standard method of CT attenuation with the use of data obtained mid expiration (78).

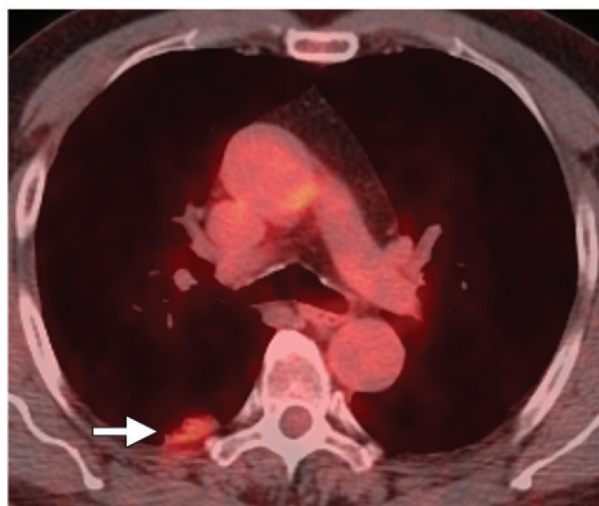
Figure 19. Focal organizing pneumonia mimicking malignancy in a 69-year-old man with esophageal cancer and a 30-pack-year smoking history. **(a)** Unenhanced CT image shows a subsolid nodule (arrow) in the right lower lobe with predominantly ground-glass attenuation. **(b)** Follow-up CT image obtained 1 year later shows the nodule (arrow), which has increased in size and attenuation. **(c)** PET/CT image shows low-grade FDG uptake in the nodule (arrow). Because of this patient's high pretest probability for malignancy (older age and history of malignancy and smoking) and imaging features (increase in nodule size and attenuation) indicative of an increased risk for malignancy, decision analysis favors biopsy. Results of transthoracic needle aspiration biopsy were negative and revealed focal organizing pneumonia.



a.



b.



c.

Decision Analysis: Management

Multiple factors, including radiation exposure, cost, limited resources, patient anxiety, and the knowledge gleaned from lung cancer CT screening trials, have contributed to the recent release of guidelines by the Fleischner Society and, more recently, the American College of Chest Physicians (ACCP), for managing solid and subsolid pulmonary nodules (3,14,79,80). Management algorithms for solid and subsolid SPNs are determined by patients' clinical risk factors and nodule characteristics. Upon completion of imaging evaluation, the goals of appropriate management are to direct clinicians to pursue a more aggressive approach for nodules that are deemed suspicious for malignancy, while sparing patients with benign nodules the morbidity and cost associated with invasive procedures to obtain tissue samples. In this regard, clinical quantitative prediction models have improved our understanding of risk factors for malignancy by determining the likelihood ratios of independent clinical and imaging

factors. Clinical factors that are determined to be significant predictors for malignancy include an older age, current or past smoking history, and a history of extrathoracic malignancy more than 5 years before nodule detection (11). Nodule characteristics associated with a higher likelihood of malignancy are size, spiculation, and an upper lobe location (81). The addition of PET results to Bayesian analysis also increases the effectiveness of the model (82).

Algorithms by the ACCP and recommendations from the Fleischner Society provide guidelines for managing solid and subsolid SPNs. In the initial evaluation, comparison with previous images is important to assess nodule growth. Solid nodules that have been stable for more than 2 years or that have a benign pattern of calcification require no further work-up. In the evaluation of nodules with an indeterminate cause after imaging, stratifying patients according to their pretest probability of malignancy is important to decide whether a nodule should be observed,

Table 4: Fleischner Society Recommendations for Follow-up of Patients with a Solid SPN

Nodule size	Risk Factor	
	Low Risk*	High Risk†
≤4 mm	No follow-up	Follow-up at 12 months
5–6 mm	Follow-up at 12 months	Follow-up at 6–12 months and 18–24 months
7–8 mm	Follow-up at 6–12 months and 18–24 months	Follow-up at 3–6 months, 9–12 months, and 24 months
>8 mm	Follow-up at 3, 9, and 24 months; consider performing contrast-enhanced CT, PET/CT, or biopsy	Follow-up at 3, 9, and 24 months; consider performing contrast-enhanced CT, PET/CT, or biopsy

*Patients who have little or no history of smoking and no other risk factors are considered low risk.

†Patients with a history of smoking or other exposure or risk factor are considered high risk.

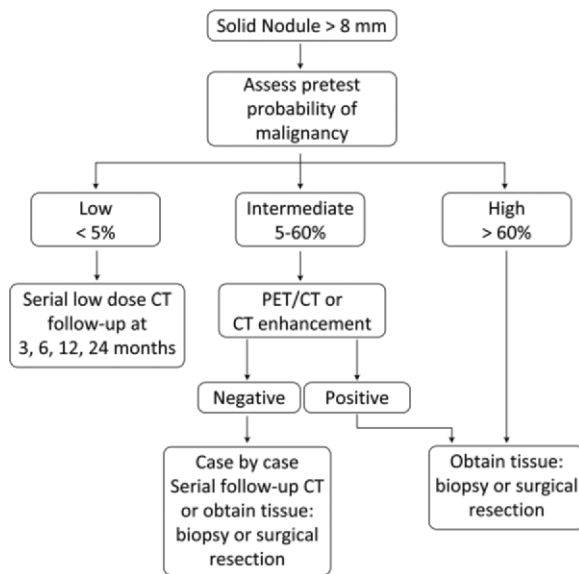


Figure 20. Flowchart shows the algorithm for evaluating solid SPNs.

biopsied, or resected. In terms of management, the decision to observe is made on the basis of the size of the nodule and its risk for malignancy. In patients with no history of cancer, fewer than 1% of nodules that are 4 mm or smaller are malignant, and no further assessment is required (Table 4). For nodules that are 5–8 mm, the frequency of serial reassessment depends on the size of the nodule and the clinical risk for malignancy, with more frequent follow-up examinations recommended for patients with a high risk for malignancy (Table 4). For solid nodules that are larger than 8 mm, stratification of patients' pretest probability for lung cancer by using clinical and morphologic risk factors determines management (Fig 20) (80). Available management options include serial reassessment at CT, performing a CT enhancement study, performing FDG PET, and performing histologic analysis to make a tissue diagnosis. For nodule reassessment, unenhanced,

thin-section, limited coverage, low-dose CT is recommended. CT enhancement studies, once considered an alternative to PET for differentiating between benign and malignant SPNs, are less widely used. It should be noted that the Fleischner Society recommendations do not apply to patients with a history of malignancy, young patients (those who are less than 35 years old and, thus, have a low risk for lung cancer), and patients with a fever because the nodules may be infectious (14).

In contrast to solid nodules, management options for subsolid nodules are less clearly defined and are limited to serial reassessment and histologic analysis to make a tissue diagnosis (Table 5, Fig 21) (3,80). CT enhancement studies are not applicable, and FDG PET is of limited use because subsolid lesions typically have low metabolic activity. Although PET should not be systematically performed in patients with a pure GGAN, it has limited use in the assessment of subsolid nodules. According to the ACCP guidelines, PET/CT may play a role in the evaluation of subsolid lesions with a solid component larger than 8 mm, and, according to the Fleischner Society guidelines, it may play a role in the evaluation of those with a solid component larger than 10 mm (3,80). One study reported that, for subsolid nodules, the finding of a solid component accounting for more than 50% of the nodule is associated with an increased risk for nodal metastatic disease (83).

According to guidelines from the ACCP and the Fleischner Society, performing thin-section CT is essential to characterize subsolid nodules in terms of any solid components, the ratio of solid-to-ground-glass attenuation, and a change in size or attenuation at serial follow-up examinations. However, these guidelines have differences (3,80). The ACCP guidelines consider pretest probability for malignancy, which is not included in the Fleischner Society recommendations. In

Table 5: Fleischner Society Recommendations for Management of Subsolid Pulmonary Nodules

Nodule size	Management Recommendations	Additional Remarks
GGAN ≤5 mm	No CT follow-up	Obtain contiguous 1-mm-thick sections to confirm that nodule is truly a pure GGAN
>5 mm	Follow-up CT at 3 months to confirm persistence, then annual surveillance CT for at least 3 years	FDG PET is of limited value, is potentially misleading, and is not recommended
PSN	Follow-up CT at 3 months to confirm persistence; if persistent and the solid component is <5 mm, yearly surveillance CT should be performed for at least 3 years; if persistent and the solid component is ≥5 mm, biopsy or surgical resection should be performed	Consider PET/CT for partly solid nodules >10 mm

addition, overall nodule size is a consideration for subsolid nodules in the ACCP criteria. In the Fleischner Society guidelines, the size of the solid portion is emphasized, but the overall nodule size is not specifically addressed if it is larger than 5 mm. These differences bring to light the challenge in managing subsolid lesions, which will be addressed as more information is accrued in terms of the natural history and significance of nodule size and other features.

For patients with a subsolid lesion, the initial 3-month follow-up at CT is to determine persistence, because lesions that result from an infectious or inflammatory cause may regress or resolve in the interval. Persistent pure GGANs that are smaller than 5 mm in diameter are typically AAH; it is unclear whether these lesions require follow-up evaluation. For persistent pure GGANs that are larger than 5 mm, continued follow-up examinations are recommended, because a small number (7%) of 5–10-mm pure GGANs can have features of invasive adenocarcinoma (84). Persistent pure GGANs that are larger than 10 mm should be assumed to be AIS or invasive adenocarcinoma, although 20%–25% will prove to be benign at resection (85). These lesions should be resected if they increase in size or attenuation or if they develop a solid component (85). If the lesion remains stable in size and attenuation, conservative management is recommended, with at least three consecutive annual thin-section CT studies to document stability. This extended period of serial reassessment CT takes into consideration the slow doubling times of adenocarcinomas (62). Because of its longer follow-up periods and large number of serial reassessments needed, imaging with a low-tube-current technique is advised to reduce cumulative radiation dose (14). For persistent subsolid nodules, management is stratified according to the size of the solid component (Fig 21). If the

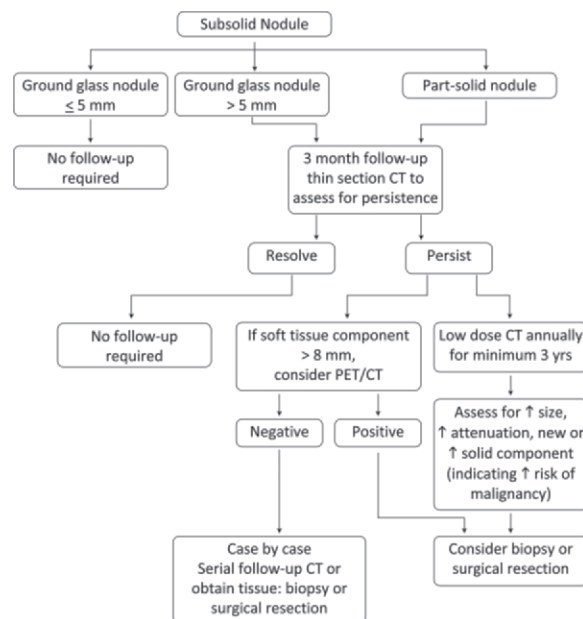


Figure 21. Flowchart shows the algorithm for evaluating subsolid SPNs.

solid component is 5 mm or smaller, follow-up imaging may be performed, whereas more aggressive management may be considered for PSNs with a solid component larger than 5 mm, as suggested by the Fleischner Society guidelines (3).

Summary

Solid and subsolid SPNs are detected with increasing frequency because of the widespread use of MDCT. Although most such nodules are benign, lung cancer is a clinically important entity in the differential diagnosis of SPNs. To ensure that appropriate treatment is initiated in a timely fashion, the aim in evaluating SPNs is to correctly differentiate malignant and benign lesions. Clinical assessment of patients' risk factors for malignancy, including age, smoking history, and history of

malignancy, is important. In terms of imaging evaluation, obtaining prior radiographs or chest CT images is useful to determine nodule growth. Further imaging evaluation, including CT enhancement studies and PET/CT, helps determine the malignant potential of solid SPNs. For solid nodules, CT enhancement of less than 15 HU and low or no FDG uptake at PET/CT suggest benignity. Awareness of potential pitfalls in nodule enhancement and PET/CT evaluation of SPNs that result from infectious or inflammatory conditions is important to avoid misinterpreting imaging findings. For subsolid nodules, CT enhancement studies are not applicable, and PET imaging is of limited use because of their low metabolic activity. Because of the likelihood that persistent subsolid nodules represent adenocarcinomas with indolent growth, serial imaging reassessment for a minimum of 3 years and/or obtaining tissue samples for histologic analysis are recommended. At imaging follow-up of subsolid nodules, growth manifesting as an increase in size, an increase in attenuation, development of a solid component, or an increase in the size of a solid component is suspicious for malignancy. Stratified according to patient risk factors for malignancy and nodule characteristics, evidence-based clinical guidelines and recommendations for the evaluation of solid and subsolid SPNs are useful in decision analysis. These management algorithms will continue to evolve as data from the lung cancer screening trials are analyzed and further studies are performed.

Disclosures of Conflicts of Interest.—S.E.R.: Activities related to the present article: disclosed no relevant relationships. Activities not related to the present article: disclosed no relevant relationships. Other activities: member of RMAN Philips advisory board.

References

- Austin JH, Müller NL, Friedman PJ, et al. Glossary of terms for CT of the lungs: recommendations of the Nomenclature Committee of the Fleischner Society. *Radiology* 1996;200(2):327–331.
- Swensen SJ. CT screening for lung cancer. *AJR Am J Roentgenol* 2002;179(4):833–836.
- Naidich DP, Bankier AA, MacMahon H, et al. Recommendations for the management of subsolid pulmonary nodules detected at CT: a statement from the Fleischner Society. *Radiology* 2013;266(1):304–317.
- Gaeta M, Volta S, Scribano E, Loria G, Vallone A, Pandolfo I. Air-space pattern in lung metastasis from adenocarcinoma of the GI tract. *J Comput Assist Tomogr* 1996;20(2):300–304.
- Lee HY, Lee KS. Ground-glass opacity nodules: histopathology, imaging evaluation, and clinical implications. *J Thorac Imaging* 2011;26(2):106–118.
- Cancer Facts and Figures 2006. American Cancer Society Web site. <http://www.cancer.org/research/cancerfactsfigures/cancerfactsfigures/cancer-facts-figures-2006>. Accessed November 6, 2006.
- Viggiano RW, Swensen SJ, Rosenow EC 3rd. Evaluation and management of solitary and multiple pulmonary nodules. *Clin Chest Med* 1992;13(1):83–95.
- Gurney JW, Lyddon DM, McKay JA. Determining the likelihood of malignancy in solitary pulmonary nodules with Bayesian analysis. II. Application. *Radiology* 1993;186(2):415–422.
- Bailey-Wilson JE, Amos CI, Pinney SM, et al. A major lung cancer susceptibility locus maps to chromosome 6q23-25. *Am J Hum Genet* 2004;75(3):460–474.
- Ginsberg MS, Griff SK, Go BD, Yoo HH, Schwartz LH, Panicek DM. Pulmonary nodules resected at video-assisted thoracoscopic surgery: etiology in 426 patients. *Radiology* 1999;213(1):277–282.
- Herder GJ, van Tinteren H, Golding RP, et al. Clinical prediction model to characterize pulmonary nodules: validation and added value of 18F-fluorodeoxyglucose positron emission tomography. *Chest* 2005;128(4):2490–2496.
- Szucs-Farkas Z, Schick A, Cullmann JL, et al. Comparison of dual-energy subtraction and electronic bone suppression combined with computer-aided detection on chest radiographs: effect on human observers' performance in nodule detection. *AJR Am J Roentgenol* 2013;200(5):1006–1013.
- Coakley FV, Cohen MD, Johnson MS, Gonin R, Hanna MP. Maximum intensity projection images in the detection of simulated pulmonary nodules by spiral CT. *Br J Radiol* 1998;71(842):135–140.
- MacMahon H, Austin JH, Gamsu G, et al. Guidelines for management of small pulmonary nodules detected on CT scans: a statement from the Fleischner Society. *Radiology* 2005;237(2):395–400.
- Henschke CI, McCauley DI, Yankelevitz DF, et al. Early Lung Cancer Action Project: overall design and findings from baseline screening. *Lancet* 1999;354(9173):99–105.
- Wahidi MM, Govert JA, Goudar RK, Gould MK, McCrory DC; American College of Chest Physicians. Evidence for the treatment of patients with pulmonary nodules: when is it lung cancer? ACCP evidence-based clinical practice guidelines (2nd edition). *Chest* 2007;132(3 Suppl):94S–107S.
- Heitzman ER, Markarian B, Raasch BN, Carsky EW, Lane EJ, Berlow ME. Pathways of tumor spread through the lung: radiologic correlations with anatomy and pathology. *Radiology* 1982;144(1):3–14.
- Winer-Muram HT. The solitary pulmonary nodule. *Radiology* 2006;239(1):34–49.
- Park CM, Goo JM, Lee HJ, Kim KG, Kang MJ, Shin YH. Persistent pure ground-glass nodules in the lung: interscan variability of semiautomated volume and attenuation measurements. *AJR Am J Roentgenol* 2010;195(6):W408–W414.
- Gurney JW. Determining the likelihood of malignancy in solitary pulmonary nodules with Bayesian analysis. I. Theory. *Radiology* 1993;186(2):405–413.
- Pinto PS. The CT halo sign. *Radiology* 2004;230(1):109–110.
- Kim SJ, Lee KS, Ryu YH, et al. Reversed halo sign on high-resolution CT of cryptogenic organizing pneumonia: diagnostic implications. *AJR Am J Roentgenol* 2003;180(5):1251–1254.
- Siegelman SS, Khouri NF, Scott WW Jr, et al. Pulmonary hamartoma: CT findings. *Radiology* 1986;160(2):313–317.

24. Muram TM, Aisen A. Fatty metastatic lesions in 2 patients with renal clear-cell carcinoma. *J Comput Assist Tomogr* 2003;27(6):869–870.
25. Siegelman SS, Khouri NF, Leo FP, Fishman EK, Braverman RM, Zerhouni EA. Solitary pulmonary nodules: CT assessment. *Radiology* 1986;160(2):307–312.
26. Swensen SJ, Yamashita K, McCollough CH, et al. Lung nodules: dual-kilovolt peak analysis with CT—multicenter study. *Radiology* 2000;214(1):81–85.
27. Seo JB, Im JG, Goo JM, Chung MJ, Kim MY. Atypical pulmonary metastases: spectrum of radiologic findings. *RadioGraphics* 2001;21(2):403–417.
28. Grewal RG, Austin JH. CT demonstration of calcification in carcinoma of the lung. *J Comput Assist Tomogr* 1994;18(6):867–871.
29. Woodring JH, Fried AM, Chuang VP. Solitary cavities of the lung: diagnostic implications of cavity wall thickness. *AJR Am J Roentgenol* 1980;135(6):1269–1271.
30. Mirtcheva RM, Vazquez M, Yankelevitz DF, Henschke CI. Bronchioloalveolar carcinoma and adenocarcinoma with bronchioloalveolar features presenting as ground-glass opacities on CT. *Clin Imaging* 2002;26(2):95–100.
31. Hansell DM, Bankier AA, MacMahon H, McLoud TC, Müller NL, Remy J. Fleischner Society: glossary of terms for thoracic imaging. *Radiology* 2008;246(3):697–722.
32. Kui M, Templeton PA, White CS, Cai ZL, Bai YX, Cai YQ. Evaluation of the air bronchogram sign on CT in solitary pulmonary lesions. *J Comput Assist Tomogr* 1996;20(6):983–986.
33. Travis WD, Brambilla E, Noguchi M, et al. Diagnosis of lung adenocarcinoma in resected specimens: implications of the 2011 International Association for the Study of Lung Cancer/American Thoracic Society/European Respiratory Society classification. *Arch Pathol Lab Med* 2013;137(5):685–705.
34. Oh JY, Kwon SY, Yoon HI, et al. Clinical significance of a solitary ground-glass opacity (GGO) lesion of the lung detected by chest CT. *Lung Cancer* 2007;55(1):67–73.
35. Koo CW, Miller WT, Kucharczuk JC. Focal ground-glass opacities in non-small cell lung carcinoma resection patients. *Eur J Radiol* 2012;81(1):139–145.
36. Kim HY, Shim YM, Lee KS, Han J, Yi CA, Kim YK. Persistent pulmonary nodular ground-glass opacity at thin-section CT: histopathologic comparisons. *Radiology* 2007;245(1):267–275.
37. Wahbah M, Boroumand N, Castro C, El-Zeky F, Eltorky M. Changing trends in the distribution of the histologic types of lung cancer: a review of 4,439 cases. *Ann Diagn Pathol* 2007;11(2):89–96.
38. Travis WD, Brambilla E, Noguchi M, et al. International association for the study of lung cancer/american thoracic society/european respiratory society international multidisciplinary classification of lung adenocarcinoma. *J Thorac Oncol* 2011;6(2):244–285.
39. Lacout A, Marcy PY, Ngo TM, El Hajjam M. Multidetector row CT scan in hypersensitivity pneumonitis: contribution of minimum intensity projection reformation. *J Med Imaging Radiat Oncol* 2011;55(3):291–295.
40. Godoy MC, Kim TJ, White CS, et al. Benefit of computer-aided detection analysis for the detection of subsolid and solid lung nodules on thin- and thick-section CT. *AJR Am J Roentgenol* 2013;200(1):74–83.
41. Park CM, Goo JM, Lee HJ, et al. CT findings of atypical adenomatous hyperplasia in the lung. *Korean J Radiol* 2006;7(2):80–86.
42. Kishi K, Homma S, Kurosaki A, et al. Small lung tumors with the size of 1 cm or less in diameter: clinical, radiological, and histopathological characteristics. *Lung Cancer* 2004;44(1):43–51.
43. Li F, Sone S, Abe H, Macmahon H, Doi K. Malignant versus benign nodules at CT screening for lung cancer: comparison of thin-section CT findings. *Radiology* 2004;233(3):793–798.
44. Austin JH, Garg K, Aberle D, et al. Radiologic implications of the 2011 classification of adenocarcinoma of the lung. *Radiology* 2013;266(1):62–71.
45. Honda T, Kondo T, Murakami S, et al. Radiographic and pathological analysis of small lung adenocarcinoma using the new IASLC classification. *Clin Radiol* 2013;68(1):e21–e26.
46. Yamada N, Kusumoto M, Maeshima A, Suzuki K, Matsuno Y. Correlation of the solid part on high-resolution computed tomography with pathological scar in small lung adenocarcinomas. *Jpn J Clin Oncol* 2007;37(12):913–917.
47. Ikeda K, Awai K, Mori T, Kawanaka K, Yamashita Y, Nomori H. Differential diagnosis of ground-glass opacity nodules: CT number analysis by three-dimensional computerized quantification. *Chest* 2007;132(3):984–990.
48. Sumikawa H, Johkoh T, Nagareda T, et al. Pulmonary adenocarcinomas with ground-glass attenuation on thin-section CT: quantification by three-dimensional image analyzing method. *Eur J Radiol* 2008;65(1):104–111.
49. Suzuki K, Kusumoto M, Watanabe S, Tsuchiya R, Asamura H. Radiologic classification of small adenocarcinoma of the lung: radiologic-pathologic correlation and its prognostic impact. *Ann Thorac Surg* 2006;81(2):413–419.
50. Tsutani Y, Miyata Y, Nakayama H, et al. Prognostic significance of using solid versus whole tumor size on high-resolution computed tomography for predicting pathologic malignant grade of tumors in clinical stage IA lung adenocarcinoma: a multicenter study. *J Thorac Cardiovasc Surg* 2012;143(3):607–612.
51. Lee HJ, Goo JM, Lee CH, Yoo CG, Kim YT, Im JG. Nodular ground-glass opacities on thin-section CT: size change during follow-up and pathological results. *Korean J Radiol* 2007;8(1):22–31.
52. Oda S, Awai K, Liu D, et al. Ground-glass opacities on thin-section helical CT: differentiation between bronchioloalveolar carcinoma and atypical adenomatous hyperplasia. *AJR Am J Roentgenol* 2008;190(5):1363–1368.
53. Fan L, Liu SY, Li QC, Yu H, Xiao XS. Multidetector CT features of pulmonary focal ground-glass opacity: differences between benign and malignant. *Br J Radiol* 2012;85(1015):897–904.
54. Gaeta M, Caruso R, Blandino A, Bartiromo G, Scribano E, Pandolfo I. Radiolucencies and cavitation in bronchioloalveolar carcinoma: CT-pathologic correlation. *Eur Radiol* 1999;9(1):55–59.
55. Gaeta M, Blandino A, Scribano E, Minutoli F, Volta S, Pandolfo I. Computed tomography halo sign in pulmonary nodules: frequency and diagnostic value. *J Thorac Imaging* 1999;14(2):109–113.
56. Kim KG, Goo JM, Kim JH, et al. Computer-aided diagnosis of localized ground-glass opacity in the lung at CT: initial experience. *Radiology* 2005;237(2):657–661.

57. Nathan MH, Collins VP, Adams RA. Differentiation of benign and malignant pulmonary nodules by growth rate. *Radiology* 1962;79:221–232.
58. Soubani AO. The evaluation and management of the solitary pulmonary nodule. *Postgrad Med J* 2008;84(995):459–466.
59. Aoki T, Nakata H, Watanabe H, et al. Evolution of peripheral lung adenocarcinomas: CT findings correlated with histology and tumor doubling time. *AJR Am J Roentgenol* 2000;174(3):763–768.
60. Friberg S, Mattson S. On the growth rates of human malignant tumors: implications for medical decision making. *J Surg Oncol* 1997;65(4):284–297.
61. Good CA. Management of patient with solitary mass in lung. *Chic Med Soc Bull* 1953;55:893–896.
62. Hasegawa M, Sone S, Takashima S, et al. Growth rate of small lung cancers detected on mass CT screening. *Br J Radiol* 2000;73(876):1252–1259.
63. Kakinuma R, Ohmatsu H, Kaneko M, et al. Progression of focal pure ground-glass opacity detected by low-dose helical computed tomography screening for lung cancer. *J Comput Assist Tomogr* 2004;28(1):17–23.
64. Revel M-P, Merlin A, Peyrard S, et al. Software volumetric evaluation of doubling times for differentiating benign versus malignant pulmonary nodules. *AJR Am J Roentgenol* 2006;187(1):135–142.
65. de Hoop B, Gietema H, van de Vorst S, Murphy K, van Klaveren RJ, Prokop M. Pulmonary ground-glass nodules: increase in mass as an early indicator of growth. *Radiology* 2010;255(1):199–206.
66. Farooqi AO, Cham M, Zhang L, et al. Lung cancer associated with cystic airspaces. *AJR Am J Roentgenol* 2012;199(4):781–786.
67. Lindell RM, Hartman TE, Swensen SJ, Jett JR, Midthun DE, Mandrekar JN. 5-year lung cancer screening experience: growth curves of 18 lung cancers compared to histologic type, CT attenuation, stage, survival, and size. *Chest* 2009;136(6):1586–1595.
68. Swensen SJ, Viggiano RW, Midthun DE, et al. Lung nodule enhancement at CT: multicenter study. *Radiology* 2000;214(1):73–80.
69. Shah SK, McNitt-Gray MF, Rogers SR, et al. Computer aided characterization of the solitary pulmonary nodule using volumetric and contrast enhancement features. *Acad Radiol* 2005;12(10):1310–1319.
70. Lowe VJ, Hoffman JM, DeLong DM, Patz EF, Coleman RE. Semiquantitative and visual analysis of FDG-PET images in pulmonary abnormalities. *J Nucl Med* 1994;35(11):1771–1776.
71. Gould MK, Maclean CC, Kuschner WG, Ryzak CE, Owens DK. Accuracy of positron emission tomography for diagnosis of pulmonary nodules and mass lesions: a meta-analysis. *JAMA* 2001;285(7):914–924.
72. Gould MK, Ananth L, Barnett PG; Veterans Affairs SNAP Cooperative Study Group. A clinical model to estimate the pretest probability of lung cancer in patients with solitary pulmonary nodules. *Chest* 2007;131(2):383–388.
73. Nomori H, Watanabe K, Ohtsuka T, Naruke T, Suemasu K, Uno K. Evaluation of F-18 fluorodeoxyglucose (FDG) PET scanning for pulmonary nodules less than 3 cm in diameter, with special reference to the CT images. *Lung Cancer* 2004;45(1):19–27.
74. Lowe VJ, Fletcher JW, Gobar L, et al. Prospective investigation of positron emission tomography in lung nodules. *J Clin Oncol* 1998;16(3):1075–1084.
75. Erasmus JJ, McAdams HP, Patz EF Jr, Coleman RE, Ahuja V, Goodman PC. Evaluation of primary pulmonary carcinoid tumors using FDG PET. *AJR Am J Roentgenol* 1998;170(5):1369–1373.
76. Yi CA, Lee KS, Kim BT, et al. Tissue characterization of solitary pulmonary nodule: comparative study between helical dynamic CT and integrated PET/CT. *J Nucl Med* 2006;47(3):443–450.
77. Beyer T, Antoch G, Blodgett T, Freudenberg LF, Akhurst T, Mueller S. Dual-modality PET/CT imaging: the effect of respiratory motion on combined image quality in clinical oncology. *Eur J Nucl Med Mol Imaging* 2003;30(4):588–596.
78. Pan T, Mawlawi O, Nehmeh SA, et al. Attenuation correction of PET images with respiration-averaged CT images in PET/CT. *J Nucl Med* 2005;46(9):1481–1487.
79. Gould MK, Fletcher J, Iannettoni MD, et al. Evaluation of patients with pulmonary nodules: when is it lung cancer? ACCP evidence-based clinical practice guidelines (2nd edition). *Chest* 2007;132(3 Suppl):108S–130S.
80. Patel VK, Naik SK, Naidich DP, et al. A practical algorithmic approach to the diagnosis and management of solitary pulmonary nodules: part 2—pretest probability and algorithm. *Chest* 2013;143(3):840–846.
81. Swensen SJ, Silverstein MD, Ilstrup DM, Schleck CD, Edell ES. The probability of malignancy in solitary pulmonary nodules: application to small radiologically indeterminate nodules. *Arch Intern Med* 1997;157(8):849–855.
82. Dewan NA, Shehan CJ, Reeb SD, Gobar LS, Scott WJ, Ryschon K. Likelihood of malignancy in a solitary pulmonary nodule: comparison of Bayesian analysis and results of FDG-PET scan. *Chest* 1997;112(2):416–422.
83. Vazquez M, Carter D, Brambilla E, et al. Solitary and multiple resected adenocarcinomas after CT screening for lung cancer: histopathologic features and their prognostic implications. *Lung Cancer* 2009;64(2):148–154.
84. Nakata M, Saeki H, Takata I, et al. Focal ground-glass opacity detected by low-dose helical CT. *Chest* 2002;121(5):1464–1467.
85. Godoy MC, Naidich DP. Subsolid pulmonary nodules and the spectrum of peripheral adenocarcinomas of the lung: recommended interim guidelines for assessment and management. *Radiology* 2009;253(3):606–622.

Update in the Evaluation of the Solitary Pulmonary Nodule

Mylene T. Truong, MD • Jane P. Ko, MD • Santiago E. Rossi, MD • Ignacio Rossi, MD • Chitra Viswanathan, MD • John F. Bruzzi, MBBCh • Edith M. Marom, MD • Jeremy J. Erasmus, MD

RadioGraphics 2014; 34:1658–1679 • Published online 10.1148/rg.346130092 • Content Codes: CH CT OI

Page 1659

Subsolid nodules contain a component with ground-glass attenuation, which is higher than that of normal lung parenchyma and lower than that of soft tissue, such as the pulmonary vessels. Subsolid nodules may have purely ground-glass attenuation, be partly solid, or have mixed solid and ground-glass attenuation (3).

Page 1660

The use of thin sections minimizes partial volume effects and the resultant misinterpretation of a small solid nodule as a subsolid lesion, which may be managed differently, and enables three-dimensional analysis, including quantitative techniques.

Page 1668

In terms of the range of volume doubling times for adenocarcinomas, tumors that manifest as a GGAN have a greater volume doubling time than do those that manifest as a PSN, which, in turn, have a greater volume doubling time than do solid lesions (60).

Page 1668

In contrast to growth in solid nodules, which is based solely on size, in subsolid nodules, growth may manifest as an increase in size, an increase in attenuation, development of a solid component, or an increase in size of a solid component. In subsolid nodules, these imaging features of growth indicate an increased risk for malignancy (Figs 10–12).

Page 1676

For patients with a subsolid lesion, the initial 3-month follow-up at CT is to determine persistence, because lesions that result from an infectious or inflammatory cause may regress or resolve in the interval.